

1N-26

31686

p31

# Prospects for Ductility and Toughness Enhancement of NiAl by Ductile Phase Reinforcement

R.D. Noebe and F.J. Ritzert  
*Lewis Research Center*  
*Cleveland, Ohio*

and

A. Misra and R. Gibala  
*The University of Michigan*  
*Ann Arbor, Michigan*

July 1991

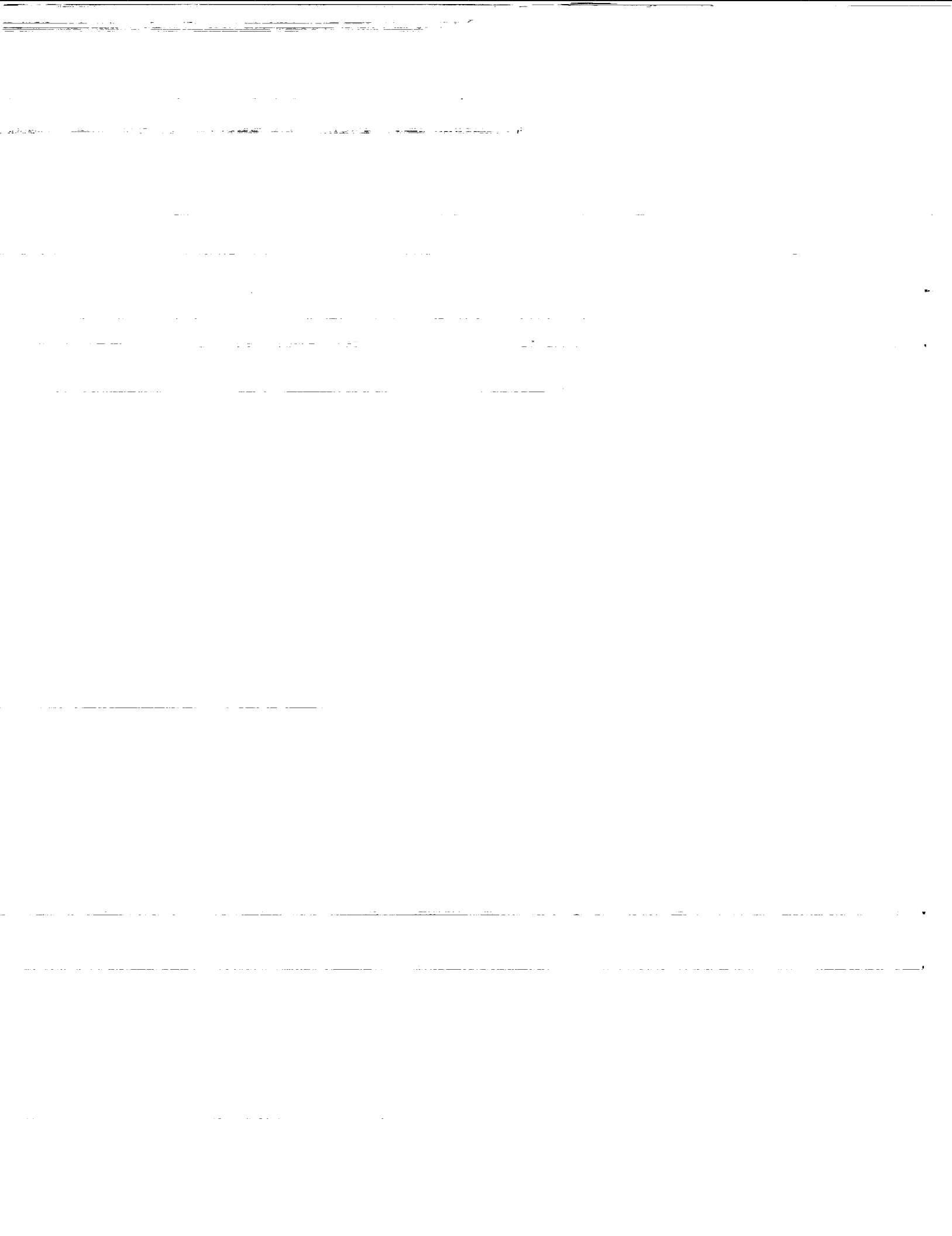


(NASA-TM-103796) PROSPECTS FOR DUCTILITY  
AND TOUGHNESS ENHANCEMENT OF NiAl BY DUCTILE  
PHASE REINFORCEMENT (NASA) 31 p CSCL 11F

N91-27324

Unclass

G3/26 0031686



# PROSPECTS FOR DUCTILITY AND TOUGHNESS ENHANCEMENT OF NiAl BY DUCTILE PHASE REINFORCEMENT

**R.D. Noebe and F.J. Ritzert**  
National Aeronautics and Space Administration  
Lewis Research Center  
Cleveland, Ohio 44135

and

**A. Misra and R. Gibala**  
Department of Materials Science and Engineering  
The University of Michigan  
Ann Arbor, Michigan 48109

## Summary

The use of NiAl as a structural material has been hindered by the fact that this ordered intermetallic does not exhibit significant tensile ductility or toughness at room temperature. A critical review of the operative flow and fracture mechanisms in monolithic NiAl has thus established the need for ductile phase toughening in this ordered system. Progress in ductile phase reinforced intermetallic systems in general and specifically NiAl-based materials has been reviewed. In addition, further clarification of the primary mechanisms involved in the flow and fracture of ductile phase reinforced alloys has evolved from ongoing investigations of several model NiAl-based materials. The mechanical behavior of these model directionally-solidified alloys (Ni-30Al and Ni-30Fe-20Al (at %)) are discussed. Finally, the prospects for developing a ductile phase toughened NiAl-based alloy and the shortcomings presently inherent in these systems are analyzed.

## 1. Introduction

The demand for new structural materials to be used in advanced jet engines and other high performance aerospace applications has been the driving force behind the development of intermetallic, ceramic and composite materials. These efforts have been necessitated primarily by the need for greater

engine operating efficiencies. This end can only be met by materials that are capable of withstanding substantially higher operating temperatures and/or possess lower densities than currently available superalloys. Furthermore, these new structural materials must exhibit ductility and toughness equivalent to that of present day superalloys at both ambient and operating temperatures, as well as possess adequate oxidation and hot corrosion resistance. This balance of properties in advanced single-crystal nickel-based superalloys is difficult to surpass. However, a serious limitation to Ni-based superalloys is imposed by the melting point of Ni<sub>3</sub>Al (1638 K) (ref. 1), which is the principal strengthening phase of these materials.

To meet the demands of ever greater engine efficiencies, alloys based on intermetallic systems have been targeted for research over the years (refs. 2 and 3). One intermetallic system which is of much interest now (refs. 4 and 5), as it was over three decades ago (refs. 6 and 7), is the B2 phase NiAl. NiAl offers a number of distinct advantages over conventional superalloys including: (1) significantly higher melting point (approximately 1950 K (ref. 8)), (2) density which is about 2/3 that of a typical superalloy (ref. 9), (3) specific modulus which is about 35 percent greater than the stiffest superalloys (refs. 10 and 11), and (4) a three- to five-fold advantage in thermal conductivity (refs. 9, 12 and 17). NiAl, when doped with trace additions of reactive elements such as Zr or Hf, also exhibits excellent isothermal oxidation resistance (refs. 13 and 14) and cyclic oxidation resistance that is superior to any existing high temperature alloy or coating material (refs. 14 to 16).

Assuming that all other properties of a NiAl alloy were comparable to a superalloy, the immediate benefits derived from using NiAl in engine applications would include reduced cooling requirements, reduced weight, and higher operating temperatures. Together these benefits would lead to increased engine thermodynamic efficiency and an increased thrust-to-weight ratio. The weight savings alone would be significant. For example, design studies have shown that the replacement of superalloy turbine blades with NiAl could lead to a 50 percent reduction in the weight of the entire rotor system of a turbine engine (ref. 5).

Unfortunately, the mechanical properties of NiAl fall short of superalloys in several critical areas. NiAl is considered unsuitable as a structural material due to its limited low temperature ductility and toughness and poor elevated temperature strength. However, recent advances in single crystal alloy development (ref. 17), and particulate (refs. 18 and 19) and continuous fiber (ref. 20) composite technologies hold promise for improving the creep strength of NiAl. Creep strengths comparable to first generation single crystal Ni-based superalloys have already been achieved (refs. 17 to 20). Unfortunately, no similar progress has been made relative to the improvement of low temperature properties of near stoichiometric NiAl. Consequently, the issue of obtaining low temperature toughness and ductility remains one of the last stumbling blocks in the development of a structural NiAl alloy.

Ductile phase reinforcement has become a common method for improving the toughness and ductility of brittle materials including NiAl. Therefore, both the low temperature behavior of binary NiAl and recent attempts at improving properties through the incorporation of a second ductile phase will be reviewed. Special emphasis will be placed on the mechanisms involved in ductile phase reinforcement, looking in some detail at the behavior of several model two phase NiAl-based alloys. Finally, both the advantages and difficulties of this approach will be discussed.

## 2. Mechanical Behavior of NiAl

Before an optimum solution to a problem can be sought it is necessary to understand not just the symptoms, which in this case are inadequate low temperature properties for NiAl, but the underlying cause of the unsuitable behavior. For NiAl, limited low temperature ductility can be traced to the flow and fracture mechanisms which are operative in this ordered intermetallic.

Considerable effort has been expended in determining the operative slip systems in near-stoichiometric NiAl single crystals (refs. 21 to 37) while additional but limited analysis has been performed on deformed polycrystalline materials (refs. 38 to 40). The general consensus of these deformation studies (summarized in table I) was that with the exception of [001] oriented single crystals, NiAl deforms by the movement of  $b = \langle 100 \rangle$  dislocations at all temperatures.  $\langle 100 \rangle$  type slip has also been justified on a theoretical basis (refs. 31, 42 to 44).

In the special case of [001] oriented single crystals the resolved shear stress for  $\langle 100 \rangle$  slip approaches zero and the stress necessary for deformation is several times greater than that for any other orientations at low and intermediate temperatures (refs. 21, 27, 32 and 41). As table I indicates, a number of different slip systems have been observed in [001] oriented crystals. The reason for this behavior has been discussed elsewhere (refs. 32 and 41).

It cannot be emphasized enough, however, that for all non-[001] single crystal orientations and polycrystalline materials, only  $\langle 100 \rangle$  slip on {011} and occasionally {001} type planes has been observed (refs. 21 to 26, 29 to 32, 37, 39 and 40). As a consequence of this preferred deformation mode, only three independent slip systems are available for polycrystalline deformation by  $\langle 100 \rangle$  slip regardless of the operative slip planes (refs. 31 and 45). Because this is less than the five independent deformation modes considered necessary for

TABLE I - OBSERVED DEFORMATION BEHAVIOR OF NiAl

Material	Temperature range, K	Slip vector	Slip plane	Analysis technique	References
Polycrystalline NiAl	300-900	$\langle 100 \rangle$	{011}	TEM <sup>a</sup>	38-40
Single crystal NiAl					
"Soft" orientations:					
[111]	77-1373	$\langle 100 \rangle$	{011}	TEM/SSTA <sup>b</sup>	21,23,30,37
[122]	77-300	$\langle 100 \rangle$	{011}	SSTA	23
[123]	77-873	$\langle 100 \rangle$	{011}	TEM	32
[110]	77-300	$\langle 100 \rangle$	{011}	SSTA/TEM	23,31
[110]	300-1373	$\langle 100 \rangle$	{001}	TEM/SSTA	21-23,26,30,37
[227]	573	$\langle 100 \rangle$	{011}	SSTA	21
[112]	77-873	$\langle 100 \rangle$	{011} or {001}	SSTA/TEM	21,25, 29
"Hard" orientation					
[001]	300-1300	$\langle 100 \rangle$	{011}	TEM/SSTA	23,27-29,32,34,35
	600-1372	$\langle 110 \rangle$	{011}	SSTA/TEM	22,23,26,32,35,37
	77-600	$\langle 111 \rangle$	{112}, {011}, or {123}	TEM/SSTA	23,25,29,32,33,36

<sup>a</sup>TEM - Transmission Electron Microscopy Investigation.

<sup>b</sup>SSTA - Surface Slip Trace Analysis.

extensive, uniform, crack free deformation of a polycrystalline aggregate (refs. 45 and 46), NiAl is considered to have little potential for exhibiting room temperature ductility (refs. 47). Experimental evidence supports this view.

In room temperature studies of NiAl (refs. 47 to 52), reported tensile ductilities have been meager, ranging from zero to a maximum of about 3 percent. Furthermore, observations (refs. 47 and 49 to 51) of grain boundary fracture in both tensile and compression specimens at low temperatures in NiAl appear to confirm that limited ductility arises from the incompatibility in the shape changes of neighboring grains due to an insufficient number of slip systems. Intergranular fracture in metals can also be due to impurity contamination of the grain boundaries. However, extensive in-situ Auger electron spectroscopy studies of cast and extruded (ref. 50) and powder extruded (ref. 54) NiAl alloys concluded that grain boundaries were clean and free from any significant impurity contamination. This would indicate that intergranular failure of NiAl is not due to impurity segregation resulting in grain boundary embrittlement. Instead, these findings support the premise that low ductility, intergranular fracture in NiAl is due to an insufficient number of operative slip systems.

NiAl is also brittle in single crystal form. Only 0.5 to 2.5 percent tensile ductility is observed below about 475 K (refs. 33 and 55) in non-[001] oriented crystals and zero ductility up to approximately 600 K in stoichiometric NiAl of near [001] orientation (refs. 33 and 56). While grain boundaries are obviously not a consideration in the deformation of single crystals, a limited number of potential slip systems can affect the ductility of an alloy such as NiAl even in single crystal form. Dislocation glide on a limited number of slip systems is not sufficient to accommodate the complex stress states that can develop near surface notches or internal defects such as inclusions, pores or shrinkage cavities. Therefore, without the means for relaxing the stress concentrations which develop at grain boundaries in polycrystalline materials or at defects in single crystals, low ductility brittle fracture can be expected in NiAl. This problem is enhanced by the poor, low temperature fracture toughness of this intermetallic.

The plane strain fracture toughness for single phase polycrystalline NiAl is only between 4 and 7 MPa $\sqrt{m}$  (refs. 57 to 61). These values are about the same as those obtained from polycrystalline ceramics, e.g., 5 to 6 MPa $\sqrt{m}$  for polycrystalline Al<sub>2</sub>O<sub>3</sub> and about 7 MPa $\sqrt{m}$  for polycrystalline Al<sub>2</sub>O<sub>3</sub>-ZrO<sub>2</sub> of eutectic composition (ref. 62). The fracture toughness of single crystal NiAl is not much better and only varies between 4 and 10 MPa $\sqrt{m}$  depending on crystallographic orientation (refs. 61 and 63).

While low fracture toughness tends to have a detrimental effect on tensile ductility, it is likely that both the poor ductility and fracture toughness of NiAl at low temperatures are a result of the operative deformation processes, i.e., <100> slip. However, a change in deformation behavior takes place at intermediate temperatures, and correspondingly NiAl undergoes a dramatic brittle-to-ductile transition in the temperature range

of 550 to 700 K (refs. 47 to 49, 51, 64 and 65). With increasing temperature the yield strength of NiAl decreases. On the other hand, the fracture strength and ductility remain essentially constant before increasing significantly in this intermediate temperature range (refs. 47 and 51). Studies (refs. 60 and 61) indicate that the fracture toughness of NiAl also increases with temperature similar to the fracture strength, as would be expected from the linear dependence between  $K_{IC}$  and fracture stress for a constant flaw size. In this intermediate temperature regime the fracture toughness of NiAl approaches 20 to nearly 50 MPa $\sqrt{m}$  depending on the microstructure and grain size (refs. 60 and 61). This behavior is definitely metallic-like in nature in contrast to the ceramic-like toughness exhibited at low temperatures.

The dramatic change in mechanical behavior at intermediate temperatures is thought to be due to the onset of thermally activated deformation processes in NiAl such as dislocation climb (refs. 31, 47 and 51). The significance of dislocation climb occurring in a material such as NiAl has been demonstrated by Groves and Kelly (ref. 66), who have determined that the combination of both glide and climb of dislocations with <100> Burgers vectors will result in five independent deformation mechanisms. This condition would satisfy the von Mises criterion for extensive plasticity in a polycrystalline material by relieving stresses at the grain boundaries and other sites of extensive stress concentration.

Consequently, the underlying cause of the poor low temperature properties of NiAl can be traced to the fact that it is a slip system limited material. To overcome this deficiency, two possibilities become immediately obvious. One approach is to alloy NiAl in such a way as to lower the ordering energy of the material so that it is possible to initiate an alternate slip system. Preliminary results (ref. 67) indicate that initiation of <111> slip in NiAl at room temperature is possible with the addition of either Cr or Mn to the intermetallic. However, these alloys still did not exhibit any room temperature ductility (ref. 67). Another approach is to add a ductile second phase to NiAl in order to increase the ductility and toughness of the composite material through extrinsic toughening mechanisms. This latter approach will be the focus of the remainder of this paper.

### 3. Ductile Phase Toughening Concepts

#### A. Macrostructural Toughening

Macrostructural toughening involves the incorporation of a ductile second phase in a brittle matrix. The purpose of the ductile phase is to interact or interfere with the progression of cracks through the matrix phase. The ductile second phase can take the form of isolated particles, interpenetrating networks or continuous phases such as lamellae or fibers. While the degree of toughening is generally dependent on the volume fraction and morphology of the second phase, the actual characteristics of the ductile phase that will generate optimum toughness have

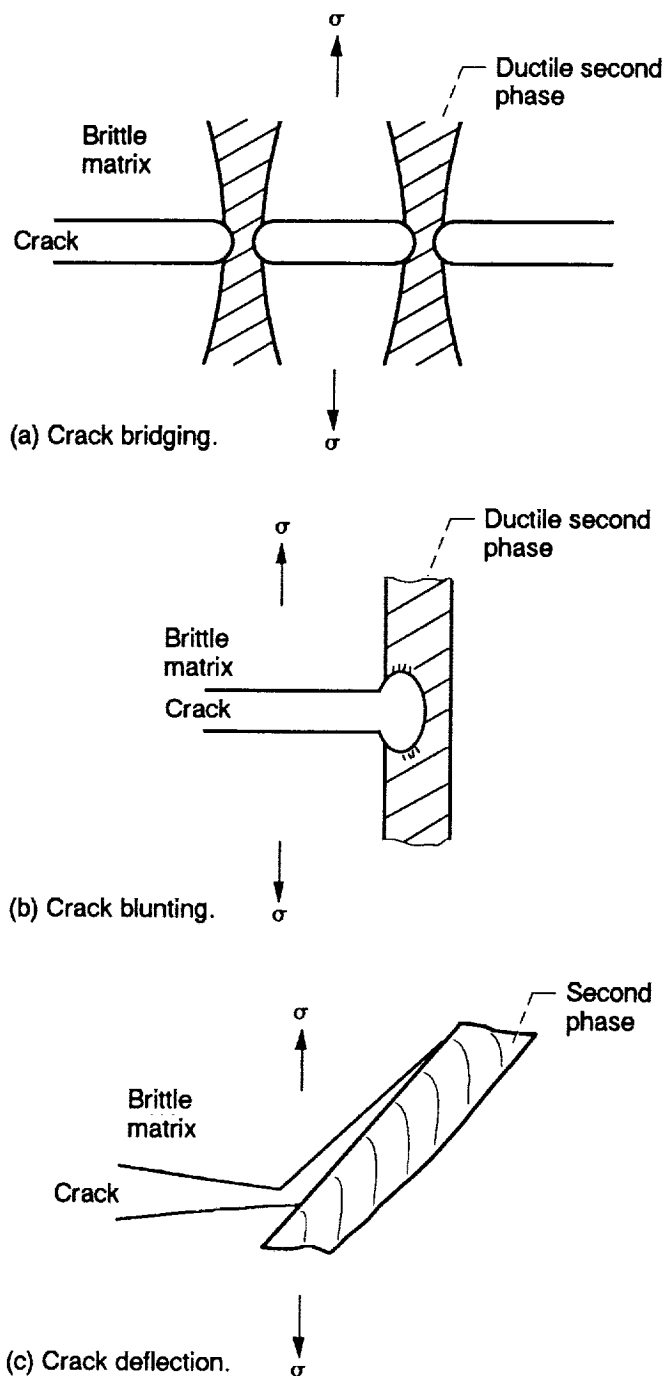


Figure 1. - Schematic illustration of the possible mechanisms for enhancing the toughness of brittle materials through the addition of a ductile second phase. (After Chan (ref. 88)).

and morphology of the second phase, the actual characteristics of the ductile phase that will generate optimum toughness have not yet been adequately established or modelled. However, much has been learned through the empirical study of ductile phase toughened systems such as glass/Al (ref. 68), WC/Co (refs. 69 and 70),  $\text{Al}_2\text{O}_3/\text{Al}$  (refs. 70 to 72),  $\text{Al}_2\text{O}_3/\text{Mo}$  (ref. 62),  $\text{MgO}/\text{Ni}$ , Fe or Co (ref. 73) and  $\text{TiAl}/\text{Nb}$  (ref. 74). From these and other studies it is evident that toughening can occur by

several different mechanisms which are generally categorized as either crack bridging, crack blunting or crack deflection. The operation of these three mechanisms is illustrated in figure 1.

During crack bridging (fig. 1(a)), moderately to strongly bonded ductile particles are intercepted by a crack which causes them to undergo extensive plastic stretching in the crack wake. This contributes to toughening by inhibiting or making further crack opening very difficult. Observations indicate that toughening by this mechanism is enhanced by increasing the volume fraction of particles present, increasing the size of the individual particles and increasing the work of rupture of the ductile second phase (refs. 70,74 and 75). In addition, toughness can be further enhanced by a ductile phase that exhibits high strength and a large strain hardening exponent and deforms uniformly instead of necking easily (ref. 74). Crack bridging would also be significantly more potent when the ductile phase is continuous in nature because the only ductile regions which experience extensive plastic strain are those segments that stretch between the crack surfaces in the bridging zone just behind the crack tip (ref. 75). Energy dissipation due to the plastic deformation in the bridged region can be quite large and provide a major increase in toughness as well as shield the crack from the external load.

In addition to serving as a bridging phase, toughening may be enhanced further by designing a ductile phase with an interface capable of undergoing limited debonding (refs. 74 and 76). This was demonstrated in one study where it was observed that energy absorption in a continuous ductile phase reinforced material increased as the length of the debond area along the bridged crack increased (ref. 76). However, extensive debonding does not result in a significant increase in steady state toughness and generally results in a decrease in the tearing modulus (ref. 74). Therefore, while some debonding along the interface may be required for optimizing energy absorption there are limits to the amount of debonding which is optimal.

A second type of bridging mechanism, which is sometimes included with crack deflection mechanisms, is the bridging of a crack by brittle fibers or whiskers. The bridging material generally has the same level of toughness as the matrix and is usually incapable of undergoing plastic deformation. By combining the two brittle components into a composite, limited toughening is achieved through interfacial debonding with crack deflection along the interface accompanied by frictional sliding along the debonded area (ref. 77). However, the degree of toughening achieved through this process is significantly less than can be realized when the bridging phase can also undergo plastic deformation.

Crack blunting (fig. 1(b)) occurs when propagation of a crack tip is impeded as it intersects a ductile particle. Through extensive localized plastic deformation of the second phase the stresses at the crack tip are relaxed sufficiently to blunt the crack and in the ideal case will prevent the crack from propagating further. Again the crack tip is shielded from the external load. A second phase material with a low yield strength will tend to maximize this effect (ref. 70).

Any second phase which exhibits a weak bond with the matrix has the potential to increase the toughness of the system through crack deflection processes. Crack deflection due to interface debonding, while not limited to ductile particles, probably contributes much less to the toughening of a component than the previous mechanisms. As illustrated in figure 1(c), the crack is redirected during the deflection process in such a way that the stress intensity at the crack tip becomes diminished (refs. 75 and 77). However, because the particle is weakly bonded to the matrix the crack will have a chance to renucleate on the other side of the second phase component. In spite of this, crack deflection is one of the easiest and most common mechanisms used to toughen ceramics (ref. 77).

Recently, ductile phase toughening has been attempted in a number of intermetallic systems with varying degrees of success (refs. 78 to 84). These studies are summarized in table II along with the toughness values of several monolithic intermetallic systems (refs. 57 to 61, 78 to 86). Crack bridging has been recognized as the major toughening mechanism in all of these ductile phase reinforced systems (refs. 78 to 84) with secondary contributions to the toughness of some of these materials due to crack deflection and crack blunting mechanisms (ref. 84).

The examples of ductile phase toughening summarized in table II are mainly laboratory-based model systems. There is, however, a successful example of the practical application of ductile phase toughening concepts, viz. the development of  $\alpha_2 + \beta$  titanium aluminide alloys (refs. 85 to 90). In this system Nb is added to  $Ti_3Al$  ( $\alpha_2$ ) in order to stabilize the formation of the more ductile high temperature  $\beta$ -phase. The  $\beta$ -phase in most cases is a disordered Nb-rich bcc phase and while it constitutes only about 10 percent of the microstructure, it exists as a continuous ductile phase (ref. 87). A typical  $\alpha_2 + \beta$  microstructure for a Ti-24Al-11Nb (at %) alloy is shown in figure 2(a). The darker phase is the disordered, ductile  $\beta$ -phase while the lighter (majority) phase is  $\alpha_2$ . Alloys of this particular composition exhibit room temperature plane strain fracture toughness values of 20 to 23  $MPa\sqrt{m}$  (refs. 84, 88 and 89), while similar alloys containing Mo and slightly higher levels of Nb can exhibit  $K_{IC}$  values of up to 30  $MPa\sqrt{m}$  (ref. 90). Tensile ductility for this family of alloys varies from about 2 percent to greater than 10 percent elongation at room temperature depending on exact composition and heat treatment (refs. 85, 88 and 90).

TABLE II. - DUCTILE PHASE TOUGHENING OF INTERMETALLIC-BASED ALLOYS

Matrix phase	Reinforcing phase (vol %)	Second phase morphology	Toughness technique	Toughness value, $MPa\sqrt{m}$	Comments	Reference
$Cr_3Si$ $Cr_3Si$	Cr(NR)	Lamellae	$K_H$ $K_H$	1-2 4-8	Ductile phase formed in-situ from the melt	78
$MoSi_2$ $MoSi_2$	Nb(10)	Continuous fibers	$K_{IC}$ $K_{IC}$	3 5	PM hot pressed material	79
$NbAl_3$ $NbAl_3$	Nb(20)	Filaments	$K_{IC}$ $K_{IC}$	1.6 9.6	Reactively hot pressed	80
$Nb_5Si_3$ $Nb_5Si_3$	Nb(>50)	Coarse particulate	$K_Q$ $K_Q$	$\leq 1$ 6-10	Ductile phase formed in-situ from the melt	81
$Nb_5Si_3$ $Nb_5Si_3$ $Nb_5Si_3$	Nb(20-60) Nb(60)	Particulate Cigar shaped particles	$K_Q$ $K_Q$ $K_Q$	3 5-15 17-27	Hot Pressed powder Blended and hot pressed power	82
$NiAl$			$K_{IC}$	4-7	Polycrystalline material	57-61
$NiAl$ $NiAl$	Mo(11) Mo(15.5)	Fine eutectic rods Eutectic rods and coarse particles	$K_Q$ $K_Q$	9.5 14	Ductile phase formed in-situ from the melt	83
$TiAl$			$K_{IC}$	~13	Single phase alloy	85,86
$TiAl$ $TiAl$	Nb(10) Ti6AL4V(16)	Pancake shaped Pancake shaped	$K_R$ $K_R$	16-20 12	Hipped plus forged composites	84

$K_{IC}$  - Plane strain fracture toughness.

$K_Q$  - Conditional fracture toughness.

$K_H$  - Toughness derived from microindentation technique.

$K_R$  - Resistance curve measurement.

NR - Not reported.

The toughness of these alloys, as in most ductile phase toughened systems, is attributed to crack bridging by the ductile  $\beta$ -ligaments (ref. 88). In addition, the  $\beta$ -phase acts as a crack blunting component and can also deflect propagating

microcracks (ref. 88). Hence, all the mechanisms described in figure 1 contribute to the toughness of  $\alpha_2 + \beta$  Ti-aluminides, although the exact contribution of each component to the toughness of these materials has not been determined.

These low temperature properties have been achieved even though  $\text{Ti}_3\text{Al}$ , like  $\text{NiAl}$ , is a slip system limited material (refs. 91 and 92). Consequently, the toughening mechanisms presented in figure 1 and the type of microstructure depicted in figure 2(a) should serve as a qualitative guide to the design of  $\text{NiAl}$ -based alloys. In fact, similar microstructures do exist in  $\text{NiAl}$ -based materials as demonstrated in figure 2(b). The development of these two phase  $\text{NiAl}$ -based alloys and their properties will be discussed in section 4.

## B. Microstructural Toughening

The constrained deformation of the ductile phase may also lead to dislocation generation at the interphase interface of the composite or two phase material and thus enable plastic deformation of the brittle matrix. Such strain transfer from the ductile second phase to the brittle matrix can be facilitated by the presence of specific orientation relationships between the two phases and a strong interphase interface. Through this mechanism additional mobile dislocations would be available to contribute to the plastic deformation of the brittle intermetallic phase and possibly postpone the initiation and/or propagation of fracture.

Theoretically, the transfer of strain from the ductile second phase to the brittle matrix can be understood by the model proposed by Clark and co-workers (ref. 93) and modified by

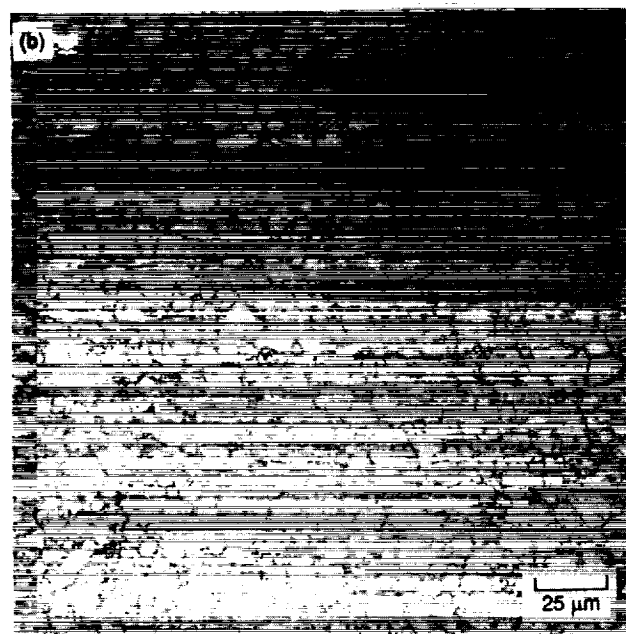
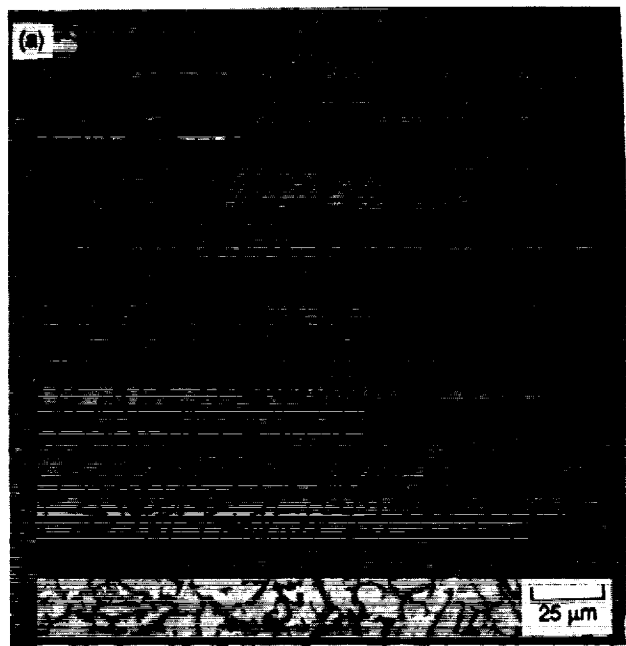


Figure 2. - Typical microstructures of tough two phase intermetallics.

- (a) Ti-24Al-11Nb Ti-aluminide composed of ordered  $\alpha_2$  (lighter majority phase) plus disordered  $\beta$ -phase.
- (b) Ni-36Al Ni-aluminide composed of  $\beta$ -NiAl (darker majority phase) plus  $\gamma$ - $\text{Ni}_3\text{Al}$ .

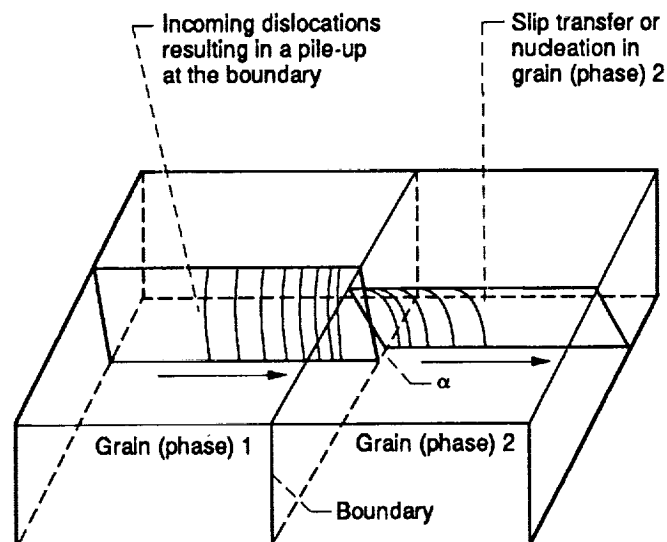


Figure 3. - Schematic illustration of strain transfer across a grain boundary or two phase interface. Dislocations approach the boundary from grain or phase 1 and either transfer through the boundary into grain 2 or are nucleated in phase 2 due to the pileup at the interface. An angle  $\alpha$  exists between the traces made by the intersection of the slip planes with the grain boundary which will be minimized by the type of slip nucleated in grain or phase 2.



Lee et al. (refs. 94 and 95) to explain slip transfer across grain boundaries in single phase materials. The situation is described schematically in figure 3, where lattice dislocations in grain (or phase) 1 approach a grain boundary (or interface) followed by subsequent initiation of slip into grain (or phase) 2. Lee et al. (refs. 95 and 96) have proposed three criteria which can be used to determine the slip system that will be activated in grain 2 by a stress concentration at the boundary due to the constrained deformation of grain 1. The slip system initiated in grain 2 will be the one for which: (1) the angle between the lines of intersection at the boundary of the incoming and outgoing slip planes will be minimized, (2) the resolved shear stress acting on the outgoing slip system from the piled-up dislocations will be maximized, and (3) the magnitude of the Burgers vector of the residual boundary dislocations generated during the slip transfer process will be minimized.

Similarly, in figure 3, if grain 1 is a ductile phase and grain 2 is the brittle intermetallic phase, then a pile-up of dislocations in phase 1 may result in slip occurring in the adjacent brittle phase. The process of deformation transfer between phases can occur by at least two mechanisms (ref. 96), either by the direct transmission of dislocations from one grain to another or by nucleation of dislocations in a neighboring grain or phase. Both processes are aided by the stress concentration at the boundary due to the pile-up of dislocations. However, direct transmission of dislocations across a boundary generally requires a dislocation reaction such that one product dislocation is transferred to the neighboring grain while a residual dislocation remains in the boundary to insure interface compatibility. While this process has been observed in single phase materials (refs. 93,94,97 and 98) it would seem improbable in two phase systems. Therefore, strain transfer between two dissimilar phases would most likely take place by nucleation of dislocations in the brittle phase as opposed to direct transfer of dislocations across the boundary.

Any transfer of strain will be facilitated by an orientation relationship between the two phases such that the angle  $\alpha$ , in figure 3, is minimized (i.e., zero or near zero). Dislocation nucleation will then occur when the resolved shear stress on the outgoing slip system from the pile-up of dislocations in phase 1 exceeds the critical value for the onset of slip. The dislocations generated at the interface will then contribute to the plastic deformation of the brittle phase, imparting additional ductility and possibly toughness to the material. However, if the interface is weak, the stress concentration due to the constrained deformation of the ductile phase may nucleate cracks at the interface and thus inhibit operation of such a mechanism. Similarly, fracture of either of the two phases would tend to inhibit the strain transfer process.

## 4. Ductile Phase Reinforced Ni-Al and Ni-Al-X Alloys

### A. Microstructural evolution

Some qualitative guidelines for choosing a ductile second phase and for the subsequent development of ductile phase toughened NiAl alloys have been discussed in section 3. Similar to the titanium aluminide alloys discussed in the previous section, one of the first places to look for an appropriate ductile phase for reinforcing NiAl is in the binary Ni-Al or a ternary Ni-Al-X system. A binary phase diagram for Ni-Al is pictured in figure 4. This is essentially the same diagram as presented by Singleton et al. (ref. 99) with the following modifications. The melting point of stoichiometric NiAl, while still thought to be congruent, is approximately 40 K greater than previously reported (ref. 8). The peritectoid reaction, resulting in the formation of  $\text{Ni}_5\text{Al}_3$ , is approximately 25 K higher in temperature (ref. 100) and the boundary for the Al-rich side of the  $\text{Ni}_5\text{Al}_3$  phase has been modified based on more recent information (ref. 101). The most significant changes in this version of the phase diagram, however, concern the  $\text{Ni}_3\text{Al}$  ( $\gamma'$ ) region. The peritectic and eutectic lines are approximately 20 K lower in temperature and the position of the eutectic and peritectic reactions are reversed. These changes are based on significant experimental work by Bremmer et al. (ref. 1) and are in agreement with previous work by Schramm (ref. 102).

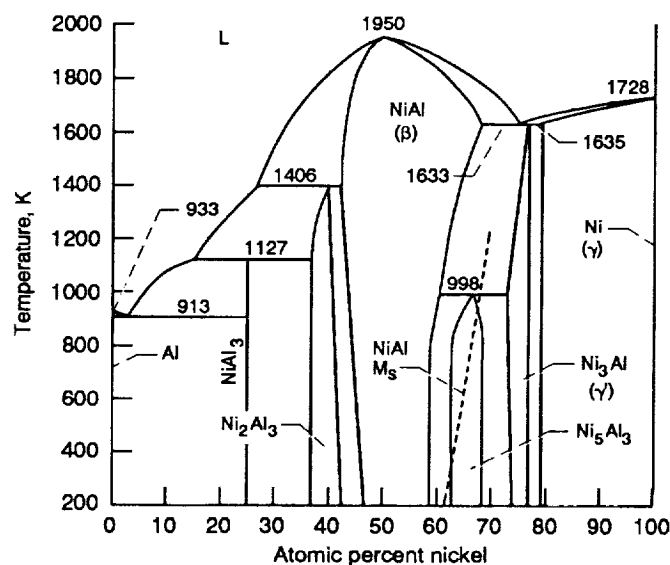


Figure 4. - Ni-Al phase diagram similar to that of Singleton et al. (ref. 99) but with several minor changes which are discussed in the text. The NiAl martensite start temperature ( $M_s$ ) is also superimposed on the plot.

It is evident from figure 4 that the only ductile phase in equilibrium with NiAl ( $\beta$ ) in the binary Ni-Al system is Ni<sub>3</sub>Al ( $\gamma'$ ) which is an ordered fcc phase. Preliminary mechanical testing has been performed on the resulting  $\beta + \gamma'$  microstructures in this binary system (refs. 103 to 105) and will be discussed shortly. Further research has been performed on two phase alloys containing ternary or higher order additions where one phase has a B2 ordered structure and the other component is either a ductile disordered fcc phase (refs. 106 and 107), a ductile ordered fcc phase (refs. 108 to 113) or combination of these two phases as a mixture of fine  $\gamma'$  particles in a  $\gamma$  matrix (refs. 114 to 116). Three excellent examples demonstrating toughening of  $\beta$ -alloys by a ductile second phase attributed to three distinctly different mechanisms may be derived from these studies.

The advantage of using Ni<sub>3</sub>Al ( $\gamma'$ ) as a ductile second phase is that it has inherent tensile ductility in single crystal form, exhibiting over 98 percent elongation at room temperature for [001] oriented crystals (ref. 117). Though Ni<sub>3</sub>Al is generally brittle in polycrystalline form because of intrinsically weak grain boundaries, this brittleness can be alleviated through microalloying additions of B (refs. 118 and 119). With B additions, the fracture toughness for Ni<sub>3</sub>Al increases from about 20 MPa $\sqrt{m}$  in the undoped condition to greater than 28 MPa $\sqrt{m}$  in B-doped material (ref. 57). Even without B additions, polycrystalline Ni<sub>3</sub>Al has superior toughness to NiAl (ref. 57). The important point is that in contrast to NiAl, Ni<sub>3</sub>Al is inherently ductile at room temperature as demonstrated by single crystal behavior (refs. 117 and 118). Furthermore, because low temperature deformation occurs by  $\langle 110 \rangle \{111\}$  slip (ref. 120), Ni<sub>3</sub>Al has enough independent slip systems (ref. 45) to accommodate plastic deformation in polycrystalline form. This makes  $\gamma'$  a good candidate for ductile phase toughening of NiAl since two phase systems can be easily formed in-situ from the melt or by proper heat treatments.

TABLE III. - PHASES WHICH HAVE BEEN OBSERVED IN BINARY Ni-Al ALLOYS CONTAINING 60 TO 70 at % Ni  
[After reference 101.]

Phase	Lattice parameter, nm	Structure type	Pearson symbol space group	References
NiAl	a = 0.2883-0.2887	B2(CsCl)	cP2 Pm3m	-----
NiAl Mart.	a = 0.383 b = 0.3205	Ll <sub>0</sub> (AuCu)	tP4 P4/mmm	122-129
Ni <sub>3</sub> Al	a = 0.3589	Ll <sub>2</sub> (Cu <sub>3</sub> Au)	cP4 Pm3m	140,141
Ni <sub>5</sub> Al <sub>3</sub>	a = 0.752 b = 0.672 c = 0.3763	Pt <sub>5</sub> Ag <sub>3</sub>	D <sub>2h</sub> <sup>19</sup> Cmmm	100,101, 122,123
Ni <sub>2</sub> Al	a = 0.407 c = 0.499	CdI <sub>2</sub>	hP3 P3m1	101,121,122

A slight complication to this approach is that a number of other stable and metastable phases can occur in the compositional region between NiAl and Ni<sub>3</sub>Al. These include the metastable phase Ni<sub>2</sub>Al (refs. 101,121 and 122), the equilibrium phase Ni<sub>5</sub>Al<sub>3</sub> (refs. 100,101,122 and 123) and NiAl martensite (refs. 101,122 to 129). The crystal structures of these phases are reviewed in table III. Fortunately, the peritectoid reaction to form Ni<sub>5</sub>Al<sub>3</sub> is extremely sluggish, requiring days or weeks to reach completion even when the aging treatment takes place within 40 K of the peritectoid temperature (refs.100 101,122 and 123). Consequently, this phase was not even identified until very recently (ref. 123). The same is true of Ni<sub>2</sub>Al (ref. 121). This phase is not observed except as a metastable phase during treatments to form Ni<sub>5</sub>Al<sub>3</sub> (refs. 101,121 and 122). Limited evidence suggests that Ni<sub>5</sub>Al<sub>3</sub> is even more brittle than NiAl (ref. 130), making it useless as a toughening agent and an undesirable phase. Therefore, it is fortunate that this phase does not occur in practice unless a very deliberate, intermediate temperature aging treatment is performed. Furthermore, Ni<sub>5</sub>Al<sub>3</sub> is not observed in ternary alloys (refs. 108 and 109) so it may be possible to eliminate this phase by alloying.

The only phase to commonly appear in the two phase composition range other than NiAl and Ni<sub>3</sub>Al is L1<sub>0</sub> NiAl-martensite. This martensitic reaction is a thermoelastic, reversible transformation which occurs when NiAl of appropriate composition is quenched below its M<sub>s</sub> temperature (refs. 101,122 to 129). The martensitic start temperature (M<sub>s</sub>) is very sensitive to chemistry and follows a very steep linear dependence on composition as the data in figure 5 indicate (refs. 58,103,124 to 129). A best linear fit of the data in figure 5 can be described by the following equation:

$$M_s (K) = 122.8 * (\text{at \% Ni}) - 7363.6$$

where the M<sub>s</sub> temperature is in degrees Kelvin and the composition of the binary alloy is entered in atomic percent Ni. The scatter of the data in figure 5 is probably more a consequence of errors in measuring composition than in M<sub>s</sub> temperature since a very slight change in chemistry results in a dramatic change in M<sub>s</sub> temperature. This dependence can be best illustrated by superimposing the fitted M<sub>s</sub> line determined from figure 5 onto the phase diagram in figure 4.

## B. Transformation Toughening

Use of the martensitic reaction has also been proposed as a mechanism for increasing the toughness of NiAl (refs. 58,59 and 131) as in TRIP steels (ref. 132) and transformation toughened ceramics (refs. 133 to 138). One of the stronger proponents for transformation toughening of NiAl-based materials is Russell et al. (refs. 59,131 and 139) who have investigated the toughness of Ni-Al and Ni-Co-Al alloys. Their single phase ternary alloys exhibited greater toughness than single phase binary Ni-Al alloys regardless of the crystal structure.

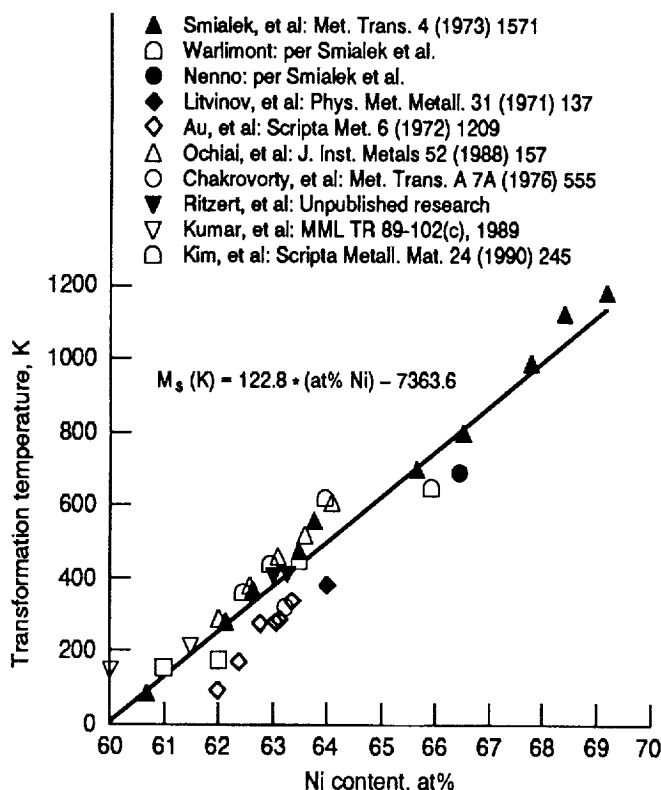


Figure 5. - The effect of composition on the martensitic transformation temperature ( $M_s$ ) for NiAl.

Both the B2-Ni-32Al-29Co and the  $L1_0$ -martensite Ni-32Al-25Co phase had similar fracture toughness values of approximately 10 MPa $\sqrt{m}$  (refs. 59 and 139). By slightly modifying the composition of these Ni-Co-Al alloys it is possible to generate a two phase microstructure containing 5 to 35 vol %  $\gamma'$ . The two phase alloys exhibited even greater toughness values in the range of 15 to 25 MPa $\sqrt{m}$  (refs. 59 and 139). Instead of being due to transformation toughening, we interpret these results as a consequence of the greater inherent toughness of the Ni-Co-Al B2 phase compared to NiAl and that ductile phase toughening mechanisms were responsible for the additional increase in toughness for the two phase materials.

Realistically, the NiAl martensitic reaction offers little benefit in the way of classical transformation toughening for this intermetallic system. In its simplest terms, transformation toughening is a process controlled by the volume increase resulting from the transforming second phase (refs. 75 and 134). The martensitic reaction which occurs in TRIP steels (ref. 132) and in  $ZrO_2$  toughened ceramics (refs. 135 to 137) results in a volume change ( $\Delta V$ ) or volume dilatation of 3 to 5 percent. Martensite formation in NiAl results in a volume change of only 0.4 percent (ref. 128). The increase in toughness due to transformation toughening ( $\Delta K$ ) is directly proportional to the volume dilatation ( $\Delta V$ ) associated with the transformation (ref. 134) and for ceramic systems, a  $\Delta V$  of 3 to 5 percent results in a  $\Delta K$  which is on the order of 5 MPa $\sqrt{m}$  (refs. 134 and 138). It follows, that because the volume increase for the

martensitic transformation in NiAl is an order of magnitude less than in these ceramic systems, the increase in toughness would also be an order of magnitude less. Therefore, transformation toughening in the NiAl system would only result in about a 0.5 MPa $\sqrt{m}$  increase in toughness, which would barely be noticed above scatter in the test results. In agreement with this argument, the toughness of  $\beta$ -phase Ni-Co-Al alloys,  $\beta$ -phase alloys which would undergo a stress induced martensitic reaction and the already fully martensitic material studied by Russell et al. (refs. 59 and 139) were the same within experimental error. Thus demonstrating that transformation toughening in NiAl-based alloys does not result in a significant increase in toughness as predicted.

### C. Necklace Microstructures as Compliant Grain Boundary Layers

From examination of the phase diagram in figure 4 it is obvious that a ductile phase reinforced intermetallic can be formed by annealing Ni-Al alloys in the two phase  $\beta + \gamma'$  region at temperatures above approximately 1000 K. The precipitation processes leading to the formation of  $Ni_3Al$  in NiAl have been studied previously (refs. 140 and 141). An example of the microstructure which results from aging a Ni-36Al alloy for 10 hr at 1000 K is shown in figure 2(b). The microstructure is similar in appearance to that of the  $\alpha_2 + \beta$  Ti-aluminide shown in figure 2(a). In the case of the Ni-aluminide sample, however,  $\gamma'$  preferentially nucleates at the grain boundaries forming a continuous film around the  $\beta$ -grains, a microstructure which is now commonly referred to as a necklace microstructure (ref. 108).

The mechanical behavior of material across the two phase field, single phase NiAl and  $Ni_3Al$  is briefly summarized in figure 6. Figure 6(a) (ref. 104) is a plot of hardness versus composition for the single and two phase Ni-aluminides, heat treated to maximize the  $\gamma'$  content in the two phase alloys. This plot gives an indication of the flow behavior for these materials. From the figure it is evident that the hardness of single phase B2-NiAl alloys increases with increasing deviation from stoichiometry for Ni-rich compositions. This increase in hardness with increasing Ni content has been observed previously by Westbrook (ref. 142). Both sets of hardness data follow the same trend as yield strength versus composition for single phase binary NiAl alloys, as summarized by Vedula and Khadkikar (ref. 143). This increase in hardness or yield strength has been attributed to defect hardening. In the off-stoichiometric alloys, excess Ni atoms will occupy Al sublattice sites which then act as "substitutional" solute atoms which cause hardening (ref. 143). Once the two phase field is reached, hardness begins to decrease rapidly as the volume fraction of the softer  $Ni_3Al$  phase increases, reaching a minimum for stoichiometric  $\gamma'$ .

Fracture toughness of Ni-Al alloys as a function of composition, taken from several references (refs. 57 to 59 and 61), is plotted in figure 6(b). From this data, it is evident that the fracture toughness for single phase NiAl is essentially independent of composition in the single phase field but begins to increase substantially in the two phase field as the percentage of  $\gamma'$  increases. The increase in toughness for the two phase alloys is a result of ductile phase toughening mechanisms.

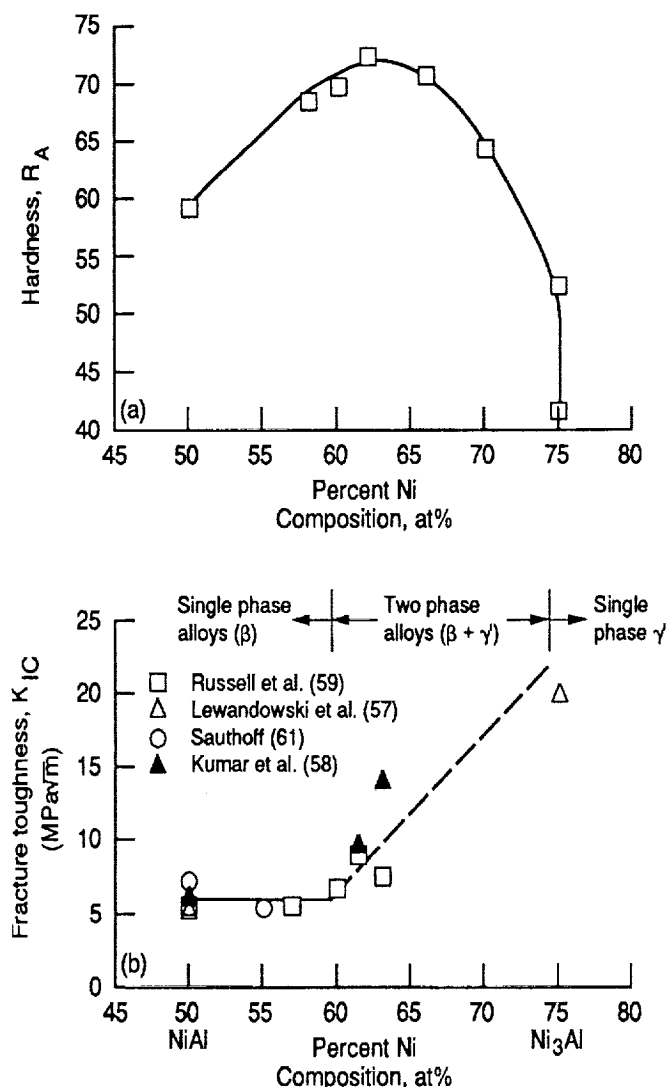


Figure 6. - The mechanical behavior of single phase and two phase Ni-Al alloys.

(a) hardness (Rockwell A scale).  
(b)  $K_{IC}$  fracture toughness.

The microstructure and bend ductility of rapidly solidified ribbons of compositions spanning the two component phase field have also been determined by Nourbakhsh and Chen (ref. 105). In qualitative agreement with the above results, they found that the bend ductility of the ribbons reached a maximum at 65 at % Ni for alloys composed of a necklace microstructure and remained roughly constant up to 75 percent Ni.

The first study identifying the possible advantages of a necklace microstructure in  $\beta + \gamma'$  alloys was performed by Pank et al. (refs. 108 and 109) on ternary Ni-Co-Al alloys. While the majority of the experiments in this investigation were performed in compression, one alloy, Ni-30Al-20Co, with a necklace microstructure exhibited 0.5 percent tensile ductility compared to essentially zero ductility for the single phase  $\beta$ -alloys. As a single phase material, Ni-30Al-20Co exists as  $L_{10}$  martensite at room temperature and even in compression at small strains exhibited extensive cracking along martensite/martensite grain boundaries. Ductility was only observed when the martensite matrix was transformed into  $\beta + \gamma'$  with the  $\gamma'$  forming a grain boundary film (refs. 108 and 109). Similar observations concerning the poor ductility of polycrystalline martensite in binary Ni-Al alloys has been made by Ritzert et al. (ref. 103).

The effect of a necklace microstructure on the tensile properties of a binary NiAl alloy is demonstrated in figure 7 (ref. 103). Figure 7(a) shows a series of stress-strain curves as a function of temperature for extruded Ni-36Al alloys in both the as-extruded condition containing only 4 percent  $\gamma'$  (fig. 7(b)) and after annealing at 1000 K for 10 hr in order to form a necklace type microstructure of  $\gamma'$  (fig. 7(c)). The BDTT for the two phase alloy composed of the necklace type microstructure occurs at a significantly lower temperature (by least 200 K) than the alloy containing only 4 percent  $Ni_3Al$ . While tensile ductility is still minimal in the two phase alloy containing 32 percent  $\gamma'$ , the room temperature fracture strength has been increased by a factor of 2.5 over that of the alloy containing very little  $\gamma'$ . Since the materials represented in figure 7 were processed identically except for the post extrusion annealing treatment, it can be assumed that the critical flaw size in these samples would be similar. Furthermore, since the test geometry was also the same for both sets of samples the 2.5-fold increase in fracture strength would, as a first approximation, correspond to a 2.5-fold increase in toughness due to the presence of the ductile second phase. This is the same order of magnitude increase in toughness as would be expected from figure 6(b) for a two phase alloy containing 64 at % Ni compared to single phase  $\beta$ -alloys.

The most recent study (ref. 107) demonstrating the advantages of a necklace microstructure in Ni-Al-X alloys is also the one which has made the most significant strides in ductility enhancement. Instead of using a compliant grain boundary layer of  $\gamma'$  as in the previous studies (refs. 59,103,108,109,139), a film of disordered  $\gamma$  phase was formed by alloying Ni-rich NiAl with either Fe, Co, Cr or Cu. The greatest room temperature ductility, nearly 10 percent, was achieved in a Ni-26Al-50Co alloy that contained 30 vol % intergranular  $\gamma$  phase. For all the two phase alloys studied by Ishida et al. (ref. 107), significant improvements in hot workability and room temperature ductility compared to single phase NiAl was attributed to the presence of the intergranular  $\gamma$  phase.

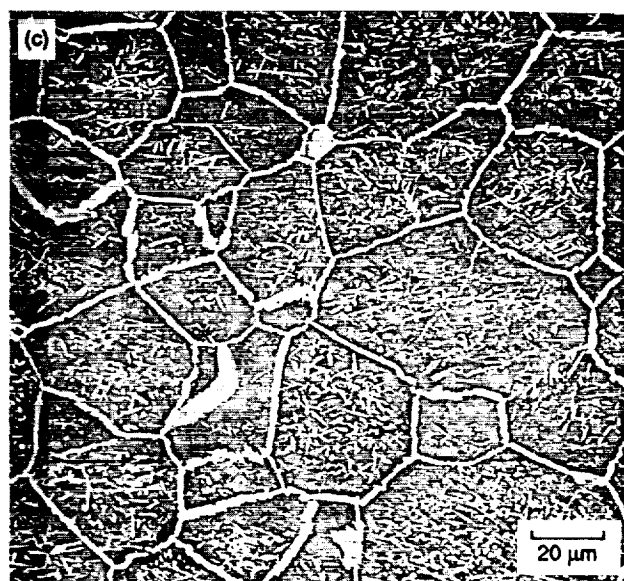
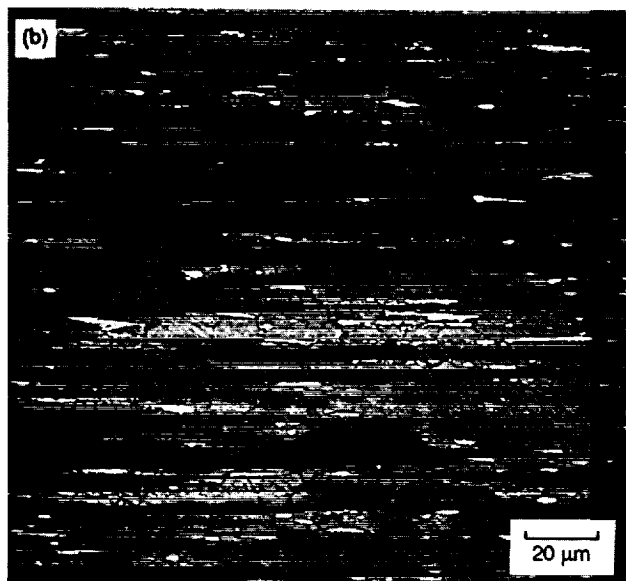
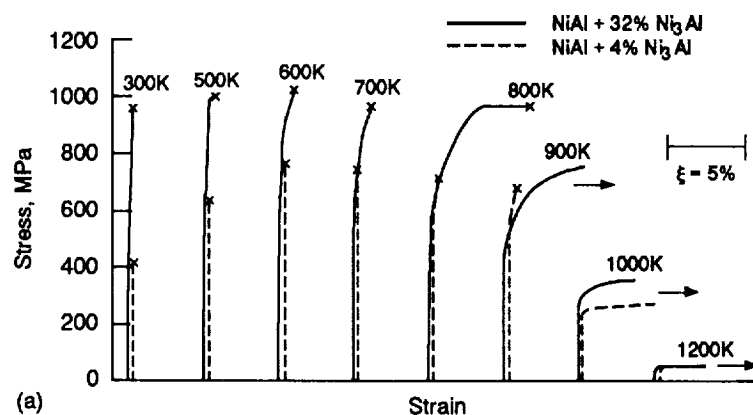


Figure 7. - The effect of microstructure on the mechanical behavior of Ni-36Al alloys.

(a) Tensile stress-strain curves as a function of temperature for Ni-Al alloys containing 4 and 32 percent  $\text{Ni}_3\text{Al}$ .

(b) Backscatter SEM micrograph of the as-extruded alloy containing approximately 4 percent  $\gamma$ .

(c) Backscatter SEM micrograph of an extruded alloy annealed at 1000 K for 10 hr resulting in a necklace microstructure of  $\gamma$ .

ORIGINAL PAGE  
BLACK AND WHITE PHOTOGRAPH

The existence of a ductile necklace microstructure in an intermetallic such as NiAl, which does not have enough slip systems to satisfy grain boundary compatibility, is beneficial because the continuous film of  $\gamma$  or  $\gamma'$  with multiple independent  $\langle 110 \rangle$  [111] slip systems enables grain-to-grain compatibility to be restored. The presence of a continuous, ductile grain boundary film thus acts as a compliant layer between grains (ref. 108). Unfortunately, the very limited tensile ductilities of alloys which exhibit  $\gamma'$  necklace microstructures (refs. 103 and 108) are at least in part due to a weak interface between the  $\beta$  and  $\gamma'$  phases (ref. 108) with fracture occurring readily along the  $\beta/\gamma'$  interface. As demonstrated in figure 6, however, toughness can still be enhanced through this type of microstructure and considerable ductility may be achieved if the interface can be strengthened. So far, significantly greater tensile ductilities have been observed with necklace structures composed of  $\gamma$  phase (ref. 107). This is possibly due to a stronger interface and the suggestion that the  $\gamma$  films are inherently more ductile than  $\gamma'$  (ref. 107).

#### D. Crack Bridging, Blunting and Deflection

Tewari (ref. 106) was one of the first investigators to make use of directional solidification processing in order to create a continuous ductile phase reinforced  $\beta$ -alloy. Directional solidification of a Ni-34.3Fe-9.9Cr-18.2Al (at %) alloy resulted in an in-situ composite consisting of alternating  $\beta$  and  $\gamma$  (disordered fcc) lamellae of approximately 40 vol %  $\beta$  phase. This "composite" material exhibited almost 17 percent tensile elongation at room temperature with fracture occurring by cleavage of the brittle  $\beta$  phase which was sandwiched between ductile necked regions of  $\gamma$ . Another remarkable aspect of this material was that cracking of the  $\beta$ -phase did not occur away from the final fracture plane. This behavior may indicate that the extensive ductility of the  $\beta$ -phase was aided by interface enhanced dislocation generation (as discussed in section 3B).

More recent work on directionally solidified, two phase microstructures and the toughening mechanisms operating in these ductile phase reinforced B2 ordered alloys has been performed by the authors. The intent of these studies is to characterize toughening mechanisms in greater detail in order to optimize them. An overview of some current results are presented below and in section 4E.

Conventional solidification of a Ni-30Al (at %) alloy produces a microstructure consisting of  $\beta$ -NiAl dendrites surrounded by interdendritic  $\gamma'$ . On cooling, the  $\beta$ -dendrites transform through solid state precipitation to  $\beta + \gamma'$ . An example of the resulting microstructure is shown in figure 8(a). Slow directional solidification of the melt (0.5 to 15 cm/hr) results in an aligned rod-like  $\gamma'$  microstructure in a single crystal NiAl matrix. The liquid solidifies as a single crystal of Ni-rich NiAl followed by solid state nucleation and directional growth of  $\gamma'$  within the single crystal parent  $\beta$ -phase (fig. 8(b)). Directional solidification at faster solidification rates

(55 cm/hr) results in an aligned dendritic microstructure as shown in figure 8(c). The bulk orientation relationship between the two phases is a Kurdjumov-Sachs relationship that was first identified by Moskovic (ref. 141) for fine Ni<sub>3</sub>Al precipitates in NiAl:

$$\begin{aligned} \langle 111 \rangle \text{NiAl} // \langle 101 \rangle \text{Ni}_3\text{Al} \\ \{011\} \text{NiAl} // \{111\} \text{Ni}_3\text{Al} \end{aligned}$$

with the growth direction of the parent NiAl phase being  $\langle 001 \rangle$ . The loading axis for all mechanical testing was parallel to the growth direction of the crystals.

The most important difference between these directionally solidified microstructures is the nature of the second phase. For example, at a solidification rate of 4.5 cm/hr, the  $\gamma'$  forms as discontinuous rods while at the slowest rate of 0.5 cm/hr the aligned  $\gamma'$  rods are essentially continuous. At much faster solidification rates the  $\gamma'$  also exists as a continuous interdendritic phase along the entire length of the crystal. In all cases the alloy contains approximately 40 percent  $\beta$ -phase and 60 percent  $\gamma'$ . The composition and properties of the individual phases have been reported previously (ref. 41) and it was determined that the  $\beta$ -phase in the two phase Ni-30Al alloy was very similar to single phase B2 Ni-40Al to which it is compared.

The particular morphology of the  $\gamma'$  phase (continuous or discontinuous) did not significantly affect the yield strength of the two phase alloy as shown in figure 9(a). Figure 9(a) also contains the yield properties of the single phase constituents which make up the two phase Ni-30Al alloy. Typical of materials containing high volume fractions of  $\gamma'$ , the yield strength of the two phase ( $\beta + \gamma'$ ) alloy increases with increasing temperature until a peak in strength is reached at approximately 875 K. While the strength of the two phase alloy is greater than single crystal  $\gamma'$  (ref. 144), it is significantly less than [001] Ni-40Al single crystals at temperatures below 800 K. This extremely low yield stress for the two phase alloy can be ascribed to the operative slip systems in the  $\beta$ -phase of both the single and two phase alloys. [001]-oriented NiAl deforms by slip of  $\langle 111 \rangle$  type dislocations at low temperatures unless the sample is mechanically unstable, in which case kinking occurs (refs. 23,25,32,33,36,41). In the deformed Ni-30Al two phase alloy,  $\langle 100 \rangle$  dislocations were observed in the  $\beta$ -phase even though the samples were mechanically loaded parallel to the [001] growth direction of the crystal. Slip by  $\langle 100 \rangle$  dislocations in the  $\beta$ -phase of the two phase alloy occurs at stresses below which macro-kinking or  $\langle 111 \rangle$  slip can occur because of the extensive operation of interfacial dislocation sources (ref. 41), similar to the microkinking model proposed by Kim et al. (ref. 36) to explain the deformation of oxide film softened NiAl. Near room temperature, this leads to a significantly reduced flow stress for the directionally solidified material compared to a rule of mixtures analysis based on the strengths of the individual components.

Unlike the yield behavior, tensile ductility of the two phase alloy is dependent on the morphology of the  $\gamma'$  phase as demonstrated in figure 9(b). When the ductile phase is continuous,

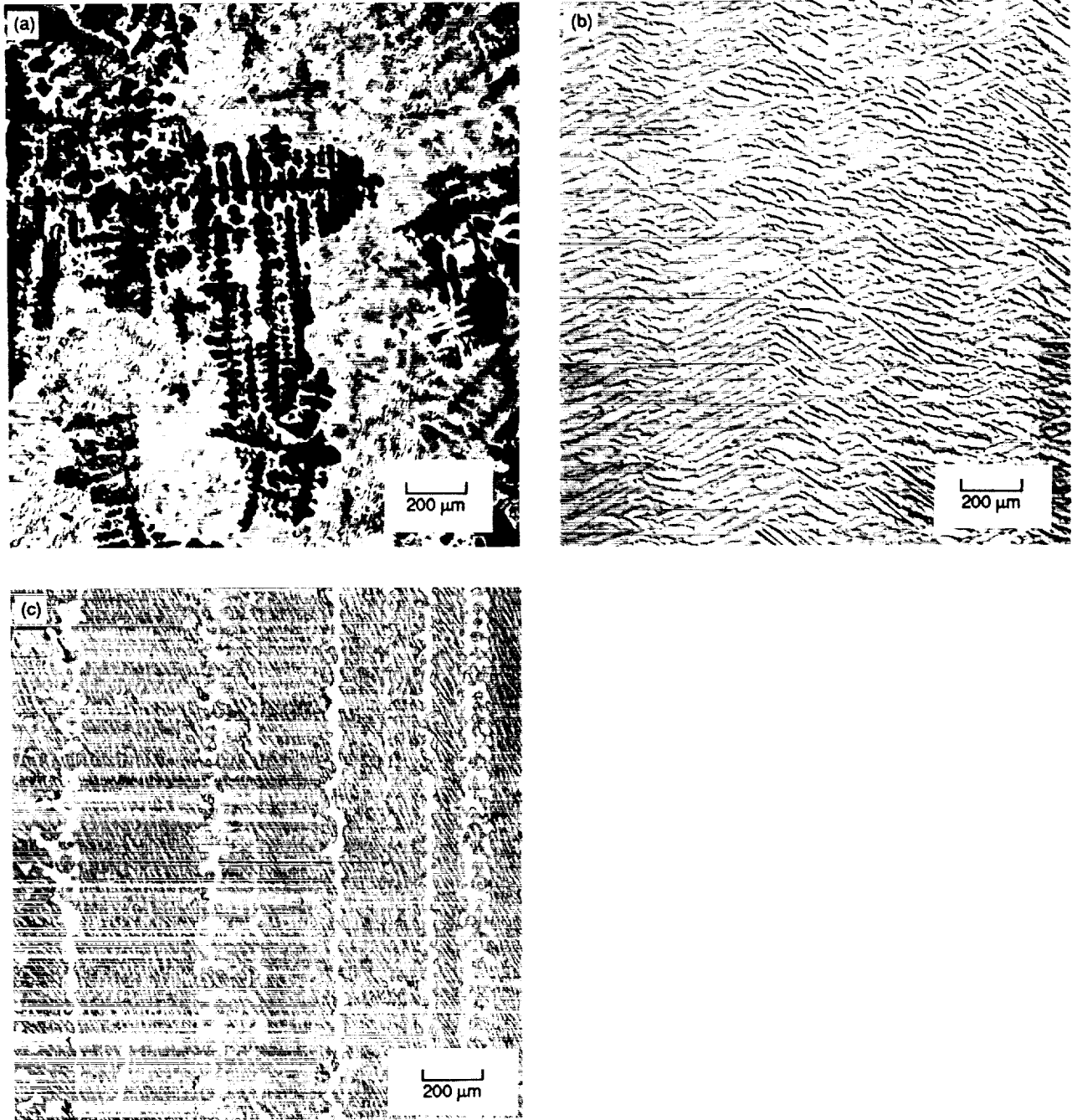


Figure 8. - Effect of processing condition on the microstructure of Ni-30Al alloys. The growth direction for figures b and c is horizontal which is also parallel to the loading direction for the mechanical test specimens.

- (a) Arc melted and chill cast alloy and longitudinal sections of material directionally solidified.
- (b) 4.5 cm/hr.
- (c) 55 cm/hr.

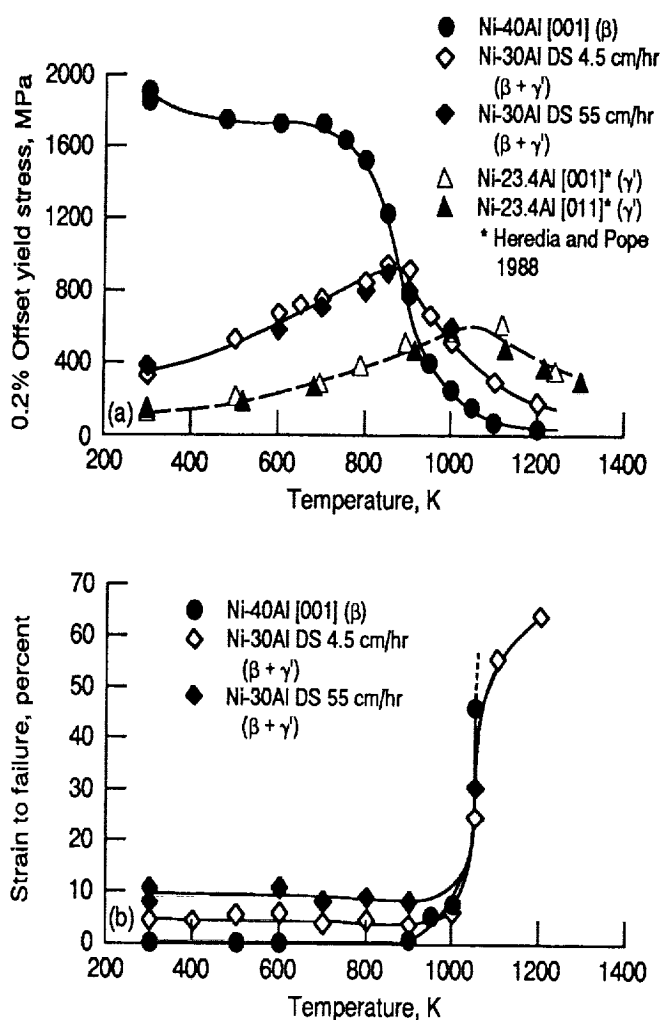


Figure 9. - Mechanical behavior of single phase, single crystal nickel aluminides and directionally solidified two phase Ni-30Al alloys as a function of temperature.

(a) Yield strength.  
(b) Tensile ductility.

as in the Ni-30Al alloy directionally solidified at a rate of 0.5 or 55 cm/hr, the tensile ductility for the material is about 10 percent at room temperature and is independent of temperature up to 1000 K. When the  $\gamma'$  phase is discontinuous as in figure 8(b), the tensile ductility of the two phase alloy is on the order of 4 percent for temperatures between 300 and 1000 K. This is still a considerable improvement over the single phase  $\beta$ -alloy which has zero ductility up to 950 K. The upturn in ductility at temperatures greater than 1000 K for the directionally solidified Ni-30Al alloy corresponds to the BDTT of the  $\beta$ -phase and the onset of ductility in that material.

The advantage of a continuous ductile phase over a discontinuous reinforcement can be understood by collectively examining figures 10 to 12. Directional solidification at 4.5 cm/hr results in discontinuous lengths of  $\gamma'$  oriented approximately  $45^\circ$  to the tensile axis (fig. 8(b)). The ductility of this alloy at room temperature is on the order of 4 percent compared to zero tensile ductility for single crystal Ni-40Al

(fig. 10). The fracture morphology of the 4.5 cm/hr directionally solidified alloy is shown in figure 11. It is apparent from figure 11(a) that secondary cracking of the  $\beta$ -phase does not occur away from the main crack plane. This implies that the  $\beta$ -phase now has some inherent ductility probably due to slip nucleation processes, as discussed previously. It is also evident from figures 11(a) and (b) that the crack did not propagate straight through the sample perpendicular to the loading direction but took a tortuous path along  $\beta/\gamma'$  interfaces. This behavior is indicative of the operation of a crack deflection mechanism. When the ductile phase is continuous (fig. 12), the crack no longer travels along the interface but is blunted by the  $\gamma'$  resulting in a tensile ductility of about 9 to 10 percent (fig. 10). While the inherent ductility of the  $\beta$ -phase has been exceeded, as evident from the extensive secondary cracking in figure 12(a), the alloy was still capable of exhibiting extensive tensile elongation due to blunting of secondary cracks and crack bridging of the main crack. Consequently, for the same volume fraction of reinforcement, increases in ductility and toughness are dependent on the morphology of the second phase, with continuous microstructures offering the largest gains in mechanical behavior. The results for the Ni-30Al alloy also indicate that in addition to crack bridging contributions, considerable toughening can occur through crack deflection and crack blunting mechanisms which can contribute to toughness in addition to the primary bridging processes.

#### E. Strain Transfer Processes

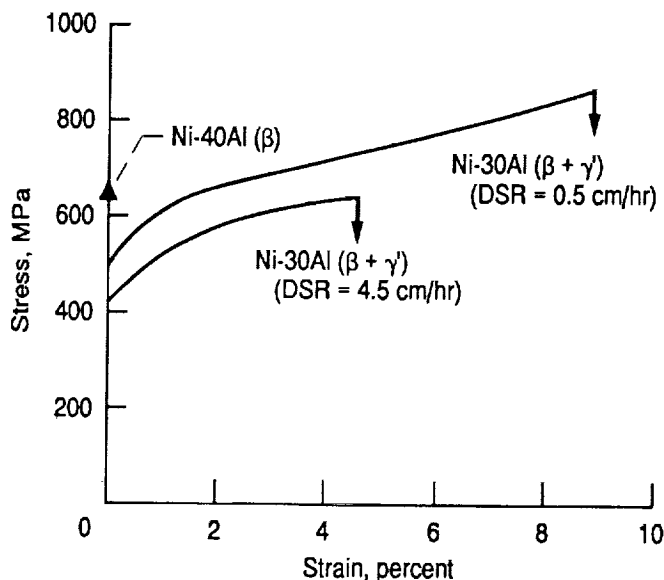


Figure 10. - Room temperature stress-strain response of two phase ( $\gamma' + \beta$ ) and single phase  $\beta$ -Ni-aluminides.



ORIGINAL PAGE  
BLACK AND WHITE PHOTOGRAPH

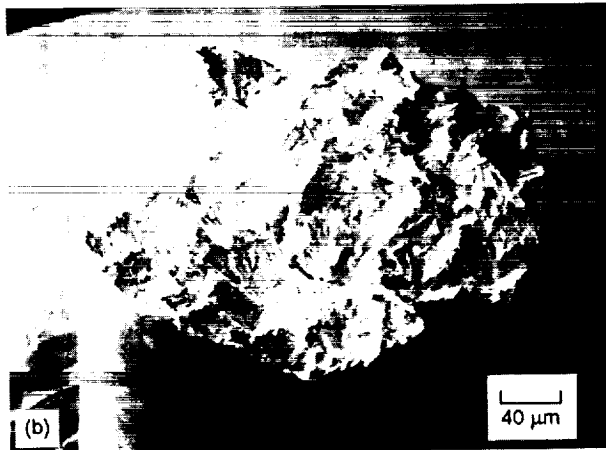
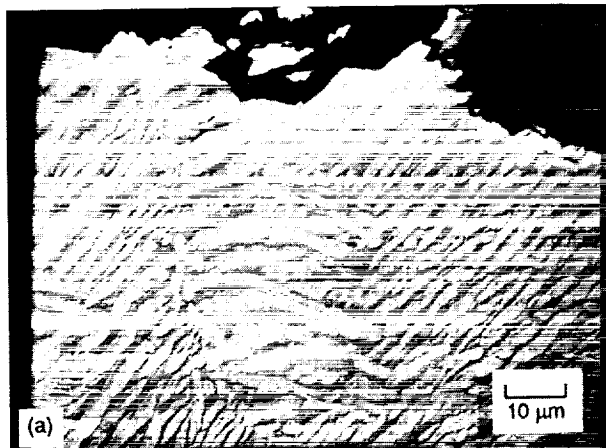


Figure 11. - Fracture behavior of a Ni-30Al alloy with a directional solidification rate of 4.5 cm/hr.

(a) Polished cross-section.

(b) Surface fracture morphology of a tensile sample indicating crack deflection as the main macrostructural toughening mechanism.

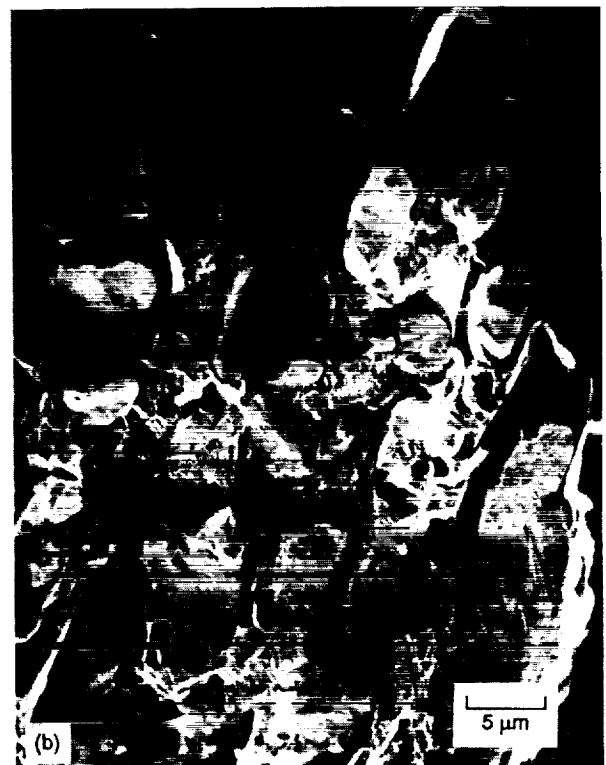
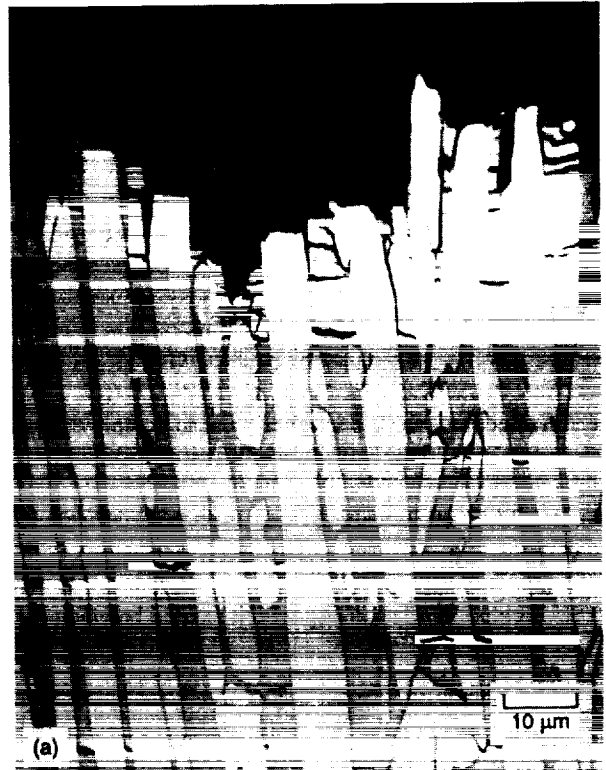


Figure 12. - Fracture behavior of a Ni-30Al alloy with a directional solidification rate of 0.5 cm/hr.

(a) Polished cross-section.

(b) Surface fracture morphology of a tensile sample indicating crack bridging and crack blunting as the main macrostructural toughening mechanisms responsible for ductility.

Ni-Fe-Al alloys consisting of an ordered bcc  $\beta$ -phase and a ductile disordered fcc  $\gamma$ -phase containing fine precipitates of  $\gamma'$  have been investigated by Huang et al. (ref. 114), Larsen et al. (ref. 115) and Guha et al. (ref. 116). The extensive ductility of these effectively two phase  $\beta + (\gamma + \gamma')$  alloys was attributed in part to the ease of slip nucleation in the  $\beta$ -phase due to slip activity in the more ductile  $\gamma$ -phase. This slip nucleation process was aided by the favorable alignment of slip systems between the two components (refs. 114 and 115). In addition to enhanced  $\langle 001 \rangle$  slip,  $\langle 111 \rangle$  slip was also observed within  $\beta$ -grains in one study (ref. 114). The occurrence of  $\langle 111 \rangle$  slip (ref. 114) may have resulted because the tougher  $\gamma$ -phase postponed fracture of the alloy long enough to allow build up of localized stresses within the  $\beta$ -phase sufficient to nucleate  $\langle 111 \rangle$  slip. Huang et al. (ref. 114) were not able to identify the source of the  $\langle 111 \rangle$  dislocations in the  $\beta$ -phase. However, nucleation of  $\langle 111 \rangle$   $\{110\}$  slip due to strain transfer from the  $\gamma$  phase was favored by the orientation relationship which existed between the two major components within the ternary alloy and could have been a likely source for these dislocations (ref. 114).

In order to study the strain transfer process in more detail an alloy with the same nominal composition, Ni-30Fe-20Al (at %), was directionally solidified to produce a brittle matrix-ductile second phase composite through eutectic solidification. The brittle intermetallic matrix was a B2 ordered  $\beta$ -phase with a nominal composition of Ni-20Fe-30Al while the ductile reinforcing phase was composed of disordered  $\gamma$ (fcc) containing fine  $\gamma'$ (L1<sub>2</sub>) particles. The nominal composition of the ductile phase was Ni-38Fe-13Al and constituted  $35 \pm 5$  vol % of the material. Details on the characterization of the individual phases are presented elsewhere (refs. 41 and 115).

The  $\beta$ -matrix phase of the composite is known to be extremely brittle in the hot extruded polycrystalline form (refs. 115,116,145). In tension,  $\beta$ -Ni-20Fe-30Al fractures after minimal ductility, 0 to 2 percent elongation (refs. 115,116,145,146), with either intergranular or transgranular fracture initiation followed by transgranular propagation (ref. 145). In compression, it was observed that deformation is only achieved through slip of  $\langle 001 \rangle$  dislocations (refs. 145 and 146). Therefore, as in NiAl, lack of extensive ductility in Ni-20Fe-30Al is attributed to an insufficient number of slip systems to meet the von Mises criterion for generalized polycrystalline ductility (refs. 45 and 46). Similarly, Ni-20Fe-30Al exhibits poor fracture toughness comparable to NiAl (ref. 147).

In contrast to the unconstrained  $\beta$ -phase, the  $\beta + (\gamma + \gamma')$  composite exhibits 10 percent tensile ductility and a 0.2 percent offset yield stress of 600 MPa when deformed at room temperature. The temperature dependence of the yield stress is similar to that observed in  $\beta$ -NiAl and other B2 alloys, i.e., a sharp increase in flow stress with decreasing temperature at low homologous temperatures, almost constant flow stress in the temperature range of  $0.15T_m < T < 0.5T_m$ , and a sharp decrease in flow stress above  $\approx 0.5 T_m$  (refs. 115 and 147).

Figures 13(a) and (b) are examples of the tensile fracture surface for the alloy. Figure 13(a) is from a region in the sample where the microstructure is lamellar and demonstrates how the ductile  $(\gamma + \gamma')$  phase mixture has necked down to a chisel edge. In contrast, the  $\beta$ -matrix exhibits a quasi-cleavage like fracture morphology. Figure 13(b) shows the fracture behavior of the same alloy in a region where the ductile phase has a rod-like morphology. In this region the ductile reinforcing phase has necked almost down to a point. Examination of the side surface of the fractured tensile specimen (fig. 14) reveals secondary cracking of the  $\beta$ -phase away from the main fracture plane. Plastic stretching of the ductile phase between the cracks is

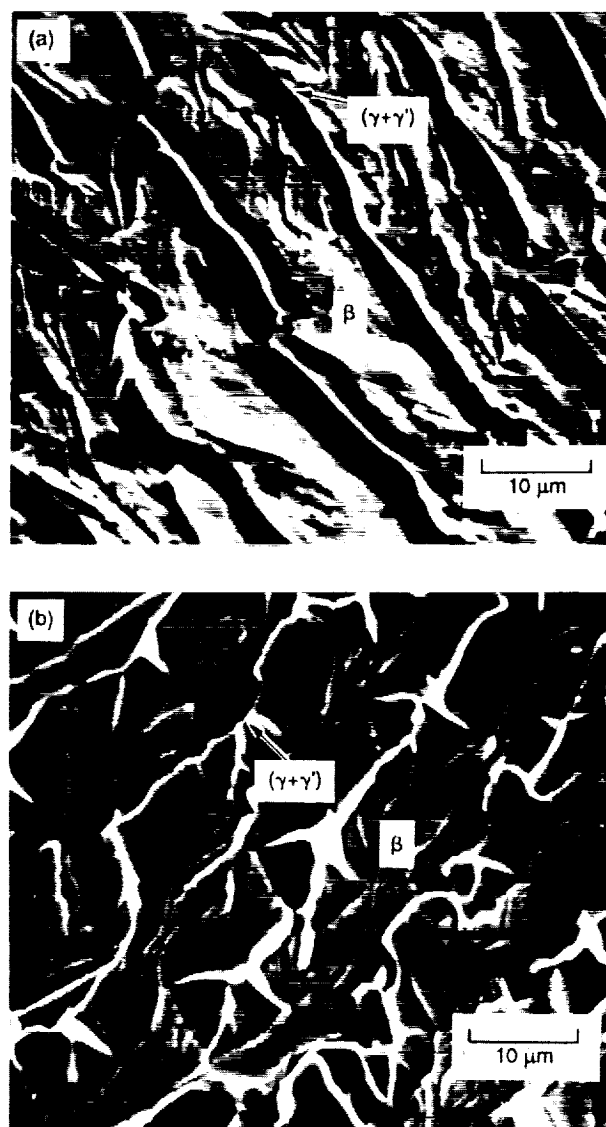


Figure 13. - Room temperature tensile fracture surface of a two phase  $\beta + (\gamma + \gamma')$  Ni-30Fe-20Al alloy.

- (a) Region of lamellar microstructure.
- (b) Region where the  $(\gamma + \gamma')$  ductile phase exhibits a rod like morphology. Extensive necking of the ductile  $(\gamma + \gamma')$  phase is evident.

quite evident while debonding along the interface is minimal. Consequently, the continuous ductile phase, as in the Ni-30Al alloy, toughens at least in part through a crack bridging mechanism.

In addition, surface observations of specimens deformed in tension at room temperature and in compression at room temperature and 77 K reveal slip traces of the type shown in

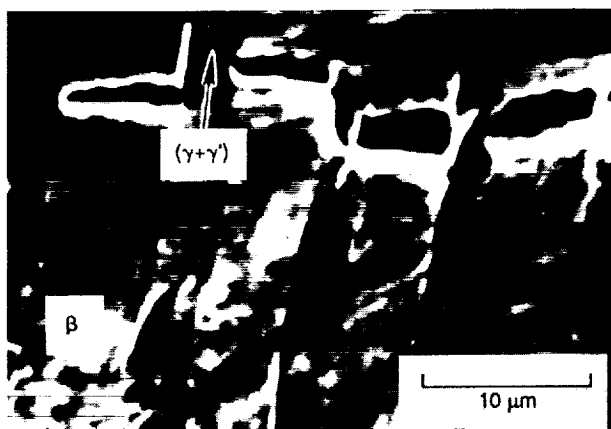


Figure 14. - SEM micrograph of the side surface of Ni-30Fe-20Al tensile specimen away from the main crack, showing how secondary cracks in the matrix have been blunted or bridged by the ductile phase.

figures 15(a) to (c), respectively. These micrographs show evidence of strain transfer from the ductile phase to the brittle  $\beta$ -matrix. The slip traces of the two phases (more readily apparent in figures 15(a) and (c)) intersect at the interface so that each slip trace in the  $(\gamma + \gamma')$  phase corresponds to a trace in the  $\beta$ -phase. The slip traces on samples deformed at 295 K are more diffuse than those observed at 77 K due to a greater propensity for the  $\beta$ -phase to exhibit cross-slip.

Transmission electron microscopy (TEM) observations of samples deformed to approximately 1 to 2 percent plastic strain in compression at 295 K confirm that deformation of the ductile phase and the strong interface play significant roles in affecting the deformation of the  $\beta$ -phase. Typical dislocation substructures observed in TEM foils cut normal to the compression axis are shown in figures 16(a) and (b). These micrographs can be interpreted as dislocation pile-ups at the interface in the  $(\gamma + \gamma')$  phase mixture leading to dislocation transfer in the  $\beta$ -phase, thus supplementing the slip trace data in figure 15 in support of the operation of strain transfer processes. In figure 16, the general slip system for the dislocations in the  $\beta$ -phase was  $\langle 001 \rangle \{110\}$  while slip in the  $(\gamma + \gamma')$  phase mixture was  $\langle 110 \rangle \{111\}$  type. Since the orientation relationship between the two phases is the same Kurdjumov-Sachs relationship observed in the Ni-30Al alloy, i.e.:

$$\begin{aligned} \langle 111 \rangle_{\beta} // \langle 011 \rangle_{\gamma} \\ \{110\}_{\beta} // \{111\}_{\gamma} \end{aligned}$$

the perfect alignment of slip planes across the boundary provides the ideal geometric condition for strain transfer (i.e.,  $\alpha = 0$  in fig. 3). Furthermore, perfect matching across each set

of surface slip traces tends to confirm the operation of a direct slip transfer process. In addition, limited evidence of  $\langle 111 \rangle \{110\}$  slip was also observed in the  $\beta$ -phase of the two phase alloy. This behavior can be attributed to the fact that the deformation axis was almost parallel to  $[001]_{\beta}$ , hence the resolved shear stress for  $\langle 111 \rangle$  slip was high; and to the Kurdjumov-Sachs orientation relationship which provides the ideal geometry for strain transfer from  $\langle 110 \rangle \{111\}$  slip in the  $\gamma$ -phase to  $\langle 111 \rangle \{110\}$  slip in the  $\beta$ -phase.

In summary, the ductility enhancement of the  $\beta$ -phase in the Ni-20Fe-30Al alloy is attributed to: (1) the inhibition of crack nucleation in the  $\beta$  due to enhanced plasticity afforded by strain transfer from the ductile second phase resulting in the increased generation of mobile dislocations and (2) the inhibition of crack propagation by plastic stretching of the ductile second phase in the crack wake, i.e., crack bridging.

## 5. Alternative Systems

While this paper is meant to be a general review of ductile phase reinforced B2 NiAl alloys, all the systems discussed so far are ones reinforced with either ordered fcc ( $\gamma'$ ) or disordered fcc phases ( $\gamma$ ). This is because almost all low temperature deformation studies of two phase NiAl-based alloys have been limited to these systems. The only exception is the NiAl-Mo eutectic alloy listed in table II. There are, however, alternative NiAl-based systems which merit study based on ternary and higher order alloying additions. These alloying additions and their effect on the microstructure of NiAl can be summarized by their position in the periodic table (ref. 148) as demonstrated in figure 17.

The elements in groups IVB and VB (Ti, V, Zr, Nb, Hf and Ta) form at least one ternary intermetallic phase with Ni and Al. The intermetallic phases most commonly observed are the Heusler phase,  $\text{Ni}_2\text{AlX}$  (refs. 56,149 to 156) and the Laves phase,  $\text{NiAlX}$  (refs. 157 to 160). These are ordered phases which are significantly more brittle than NiAl alloys and would therefore preclude the development of a ductile phase toughened alloy. However, NiAl/Heusler (refs. 150 and 156) and NiAl/Laves (refs. 157 to 160) alloys are still being actively investigated because of their superior elevated temperature creep strength compared to single phase NiAl alloys.

ORIGINAL PAGE  
BLACK AND WHITE PHOTOGRAPH

ORIGINAL PAGE  
BLACK AND WHITE PHOTOGRAPH

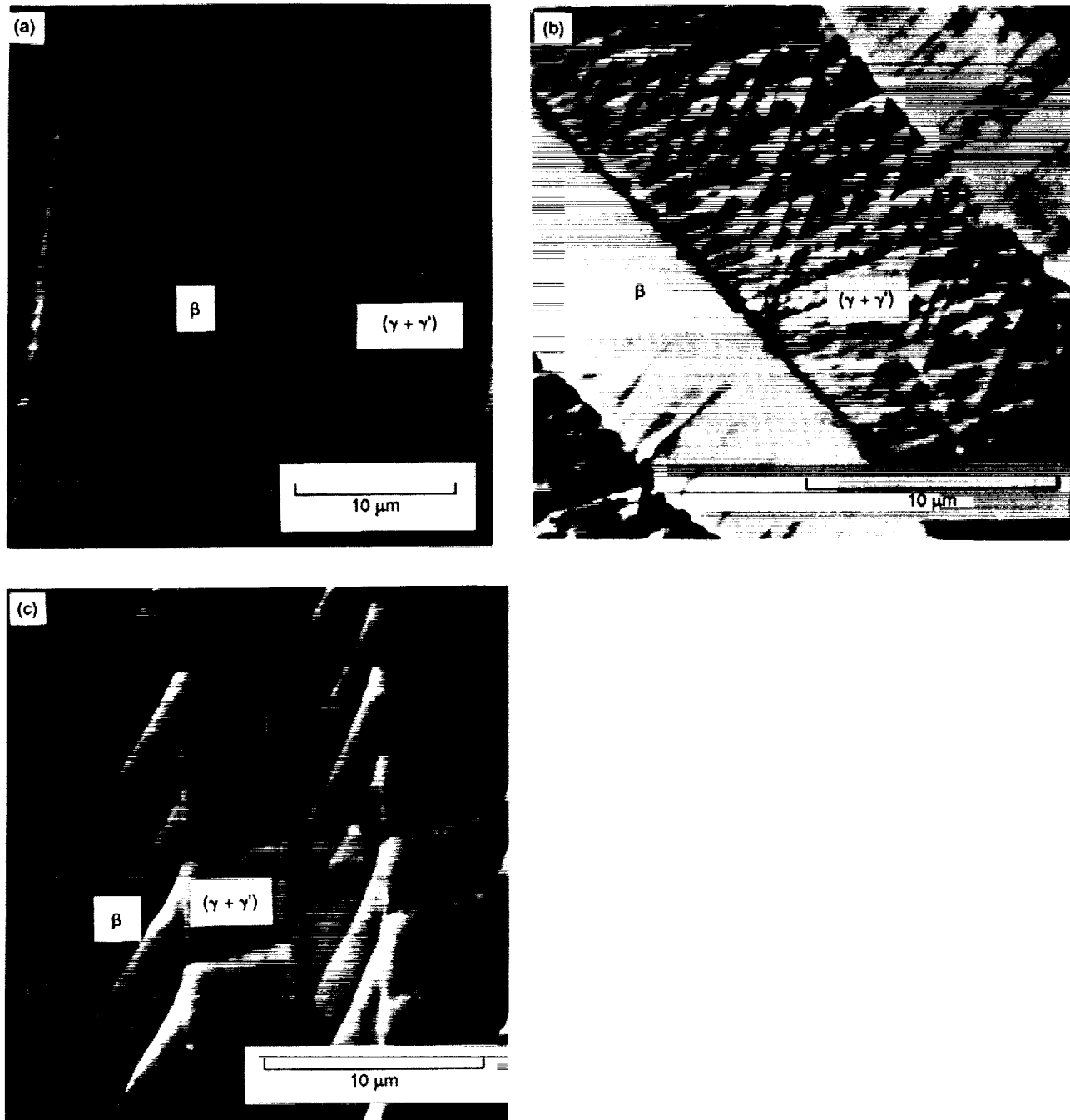


Figure 15. - SEM micrographs of slip traces in Ni-30Fe-20Al.

(a) Tensile specimen fractured at 295 K.

(b) Compression specimen deformed to 19 percent strain at 295 K.

(c) Compression specimen deformed at 77 K to approximately 15 percent strain. All three figures demonstrate strain transfer from the ductile  $(\gamma + \gamma')$  phase to the  $\beta$ -phase.

ORIGINAL PAGE  
BLACK AND WHITE PHOTOGRAPH

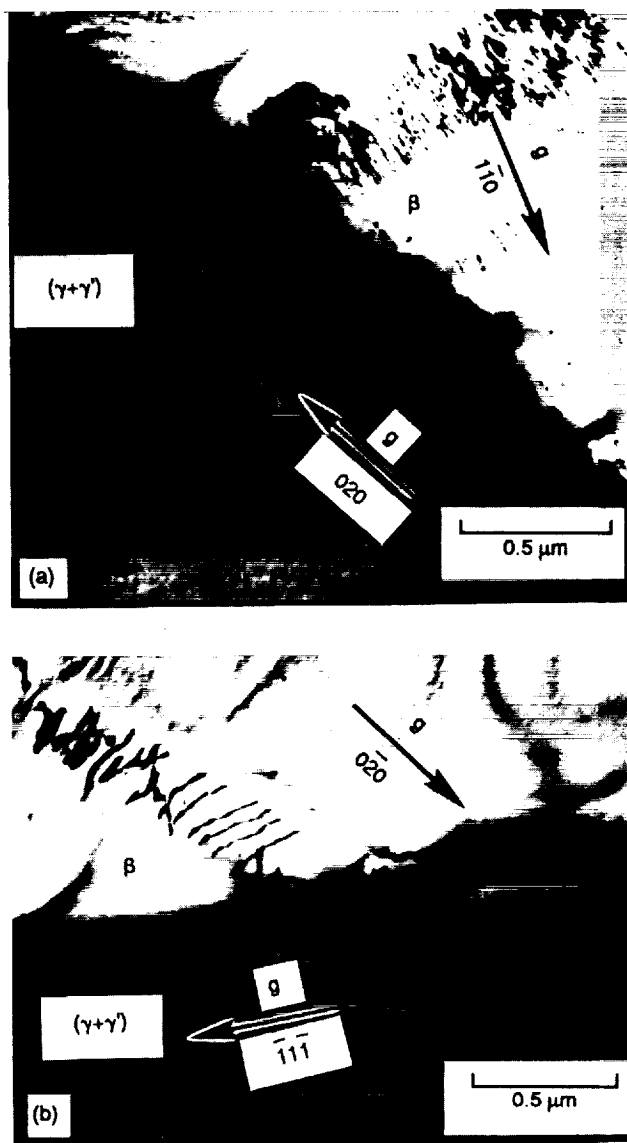


Figure 16. - (a) and (b) Bright field TEM micrographs which show the nucleation of dislocations in the  $\beta$ -phase due to dislocation pileups in the ductile  $(\gamma + \gamma')$  phase.  $\bar{B} = [001]$  for  $\beta$  and  $[\bar{1}01]$  for the  $(\gamma + \gamma')$  in both micrographs.

IIIB	IVB	VB	VIB	VIIB	VIII				IB	IIB
Sc	Ti	V	Cr	Mn	Fe	Co	Ni	Cu	Zn	
Y	Zr	Nb	Mo	Tc	Ru	Rh	Pd	Ag	Cd	
La	Hf	Ta	W	Re	Os	Ir	Pt	Au	Hg	



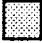
	Intermetallic (Heusler or Laves) phase formation
	Pseudobinary eutectic
	High solubility in NiAl, often isostructural

Figure 17. - Portion of the Periodic Table of Elements illustrating the general effect of ternary alloying additions on the microstructure of NiAl. (After Cotton (ref. 148)).

Groups VIB and VIIB refractory metal elements (Cr, Mo, W, and Re) in addition to V exhibit very little solubility, 1 percent or less, in NiAl and form no ternary intermetallic phases (with the exception of V). Instead, these elements form pseudobinary eutectic systems with NiAl (refs. 65,83,153,161 to 169) and therefore have the potential for in-situ ductile phase reinforcement. These  $\alpha + \beta$  systems would be obvious candidates for ductile phase toughening experiments, however, only three preliminary studies have reported room temperature properties for NiAl-refractory metal systems. Subramanian et al. (ref. 83) observed toughness increases in NiAl-Mo eutectic and hypereutectic compositions, due to crack bridging by the more ductile  $\alpha$ -Mo phase (table II). Walter and Cline (ref. 161) performed a limited number of tensile tests on directionally solidified NiAl-Cr eutectics and found that the in-situ composites were completely brittle at room temperature but did exhibit tensile ductility at 973 K and above. In the last study, NiAl-Re alloys tested in tension exhibited zero ductility from 300 to approximately 900 K (ref. 65). While no increase in ductility or toughness was observed in this system, it should be noted that the Re was distributed in the matrix as a small volume fraction of very fine discrete particles and did not exist in a geometry which would lead to toughening.

These preliminary studies raise several issues concerning refractory metal containing eutectic systems. One issue is the volume fraction of second phase available for reinforcement. The volume fraction of Re present at the NiAl-Re eutectic composition is only about 2 percent (ref. 167). While Budberg (ref. 169) reported that the eutectic composition for NiAl-W would result in approximately 17 vol % W, it is now felt that the eutectic composition previously reported (ref. 169) is in error and that the NiAl-W eutectic like the NiAl-Re system would only possess several volume percent refractory metal phase (ref. 166). This problem, however, can be overcome by working at hypereutectic compositions.

Another concern with refractory metal containing systems is the ductility or toughness of the refractory metal reinforcement. For instance, V is severely embrittled by the presence of Ni or Al (ref. 170) and would be inadequate as a ductile second phase

in NiAl unless some quaternary addition can be found to reverse these effects (ref. 171). Consequently, the most promising eutectic system seems to be NiAl-Mo though additional work needs to be performed on the NiAl-Cr and the other eutectic systems.

Many of the group VIII and IB elements (Fe, Co, Cu, Ru) plus Mn are isostructural with NiAl to varying degrees. These elements often display a large solubility in NiAl (refs. 106 to 116,172 to 177) and offer a considerable alloying potential which is mainly unexplored at this time. Ductile phases such as ordered  $L1_2$  ( $\gamma'$ ) and especially disordered fcc phases ( $\gamma$ ) also exist within these ternary systems (refs. 102,106 to 114,165,176 and 177).

In general, however, any Ni-rich NiAl-X alloy will contain some ductile phase either as  $\gamma$  or  $\gamma'$ . The elements Fe, Co, Cr, Cu and Mn tend to stabilize  $\gamma$ -phase formation in  $\beta$ -alloys, while Ta, Ti, W, V, Mo and Nb tend to stabilize  $\gamma'$  formation in Ni-rich NiAl alloys (ref. 107). As a rule of thumb, the  $\gamma'$ -phase is stabilized by elements which have a low solubility in the  $\beta$  phase and much greater solubility in  $\gamma'$ . The  $\gamma$ -phase seems to be stabilized by those elements which to some extent are isostructural with NiAl. With the exception of Ni-Al-Co ternary alloys (refs. 59,107 to 109,139) and recent work on the Ni-Fe-Al system (refs. 107,114 to 116), ternary or higher order ductile phase reinforced alloys have not been significantly investigated.

In principle, an inexhaustible source for ductile phase toughening of NiAl is the fabrication of "artificial" composites. This would include everything from the creation of laminates, to fiber reinforced composites to what is known as microstructurally toughened (refs. 76 and 178) composite systems. Presently, only limited work on NiAl-based materials has been conducted in this area. In one such investigation, continuous fiber reinforced NiAl composites were successfully produced (refs. 179 and 180). During this work it was discovered that the room temperature bend ductility of composites containing sapphire fibers was improved over that of monolithic NiAl. This increased bend ductility was primarily attributed to crack bridging by the brittle  $Al_2O_3$  fibers.

More impressive results have been achieved by Nardone et al. (refs. 76 and 178) on what they refer to as microstructurally toughened composites. Within the context of this review, these composites are more appropriately classified as macrostructurally toughened components, created by reinforcing NiAl with 304 stainless steel. A typical specimen contained about 40 vol % 304 stainless steel and was consolidated by extrusion. The room temperature mechanical properties for these composites were outstanding. The notched impact energy absorption was 15 to 90 J/cm<sup>2</sup> compared to 0.8 J/cm<sup>2</sup> for monolithic NiAl, while the tensile strain to failure for the composites was on the order of 20 to 35 percent.

The room temperature mechanical properties for these composites were outstanding. The notched impact energy absorption was 15 to 90 J/cm<sup>2</sup> compared to 0.8 J/cm<sup>2</sup> for monolithic NiAl, while the tensile strain to failure for the composites was on the order of 20 to 35 percent.

Fabrication of artificial composite systems can lead to an infinite number of composite combinations simply by varying the type of toughening agents as well as the geometry, size and volume fraction of the reinforcing materials and should be a fruitful area of research for years to come.

## 6. Caveats Pertaining to Ductile Phase Toughening Approaches

So far, a favorable view of ductile phase toughening has been presented. Unfortunately, all NiAl-based systems described in this paper as examples of various toughening concepts suffer from new problems which severely compromise their perceived usefulness. The admirable properties of NiAl were described in some detail in the introduction of this paper (e.g., melting point, environmental resistance, density, thermal conductivity, etc.). These advantages must not be lost in a ductile-phase toughened NiAl component or the driving force for its use disappears. For example, the use of  $\gamma'$  as a reinforcing agent depresses the melting point of the NiAl-based material to that of typical superalloys, eliminating the original temperature advantage and significantly reducing the density advantage of NiAl.

As stated in the introduction of this paper, binary NiAl suffers from very poor elevated temperature creep strength which is at least an order of magnitude lower than a first generation single crystal Ni-base superalloy (fig. 18). Moreover, reinforcing NiAl with a soft, low temperature ductile phase will probably reduce creep strength even more. For example, the creep strength of a number of nickel-aluminide materials are presented in figure 18, and are compared in table IV, including several of the materials highlighted in this paper, e.g., polycrystalline Ni-36Al with a necklace  $\gamma'$  microstructure and directionally solidified Ni-30Al. In both cases, the creep strength of the two phase alloys is significantly lower than binary NiAl in either single crystal or polycrystalline form. Consequently, some type of high temperature reinforcing phase will also have to be incorporated into these ductile phase toughened systems or a more judicious choice of reinforcing phase will have to be made. For example, instead of  $\gamma'$ , Mo could be used as a reinforcing agent. Molybdenum not only has a high melting point (2890 K) but certain Mo alloys are extremely creep resistant (ref. 181). Molybdenum is also thermodynamically compatible with NiAl, a factor that has to be taken into account when producing artificial composites with binary NiAl. Therefore, while the room temperature results of Nardone et al. (refs. 76 and 178) are very encouraging, compatibility problems would occur in the NiAl/304 stainless steel composites at temperatures even below that where creep strength would be the limiting factor.

Finally, the cyclic oxidation resistance of NiAl-based materials would almost certainly be degraded in ductile phase

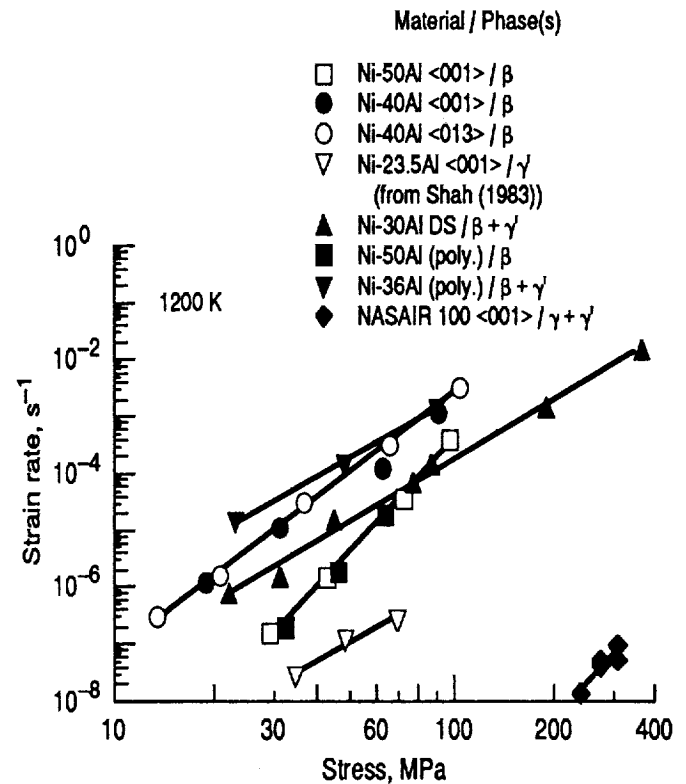


Figure 18. - The creep strength of various nickel aluminides and a first generation single crystal superalloy at 1200 K. (After Bowman et al., (ref. 33)).

TABLE IV. - COMPARISON OF THE 1200 K CREEP PROPERTIES OF VARIOUS NICKEL ALUMINIDES AND A FIRST GENERATION NI-BASE SUPERALLOY

Material, at % <orientation>	Phases(s)	Stress exponent, $n$ , $\dot{\epsilon} = K\sigma^n$	Stress (MPa) to produce $\dot{\epsilon} = 10^{-7} s^{-1}$
Ni-50Al <001>	$\beta$ -NiAl	6.4	30
Ni-40Al <013> or <001>	$\beta$ -NiAl	4.8	11
<sup>a</sup> Ni-23.5Al <001>	$\gamma'$ -Ni <sub>3</sub> Al	3.3	50
Ni-30Al (directionally solidified 4.5 cm/hr)	$\beta + 60\% \gamma'$	3.6	13
Ni-50Al (polycrystalline)	$\beta$ -NiAl	6.7	30
Ni-36Al (polycrystalline-necklace structure)	$\beta + 32\% \gamma'$	3.2	5
NASAIR 100 <001>	$\gamma + \gamma'$	7.2	300

<sup>a</sup>Shah, 1983 (ref. 183).

toughened systems. NiAl has outstanding cyclic oxidation resistance when doped with rare earth elements because of the tenacity of the  $\text{Al}_2\text{O}_3$  scale which forms during oxidation and its resistance to spalling (refs. 14,15, and 182). This behavior, however, is extremely sensitive to the stoichiometry of NiAl as demonstrated in figure 19. When the composition of single phase NiAl varies by as little as 5 at % Ni from the equiatomic composition, the long term cyclic oxidation resistance of the alloy begins to degrade due to the formation of non- $\text{Al}_2\text{O}_3$  oxides. This problem is aggravated in the two phase ( $\beta + \gamma'$ ) composition regime which is the region of interest for ductile phase toughened alloys. A simple solution to this problem would be the application of an oxidation resistant coating to the toughened alloy. Coating compatibility and integrity then become additional issues which need to be addressed during component development.

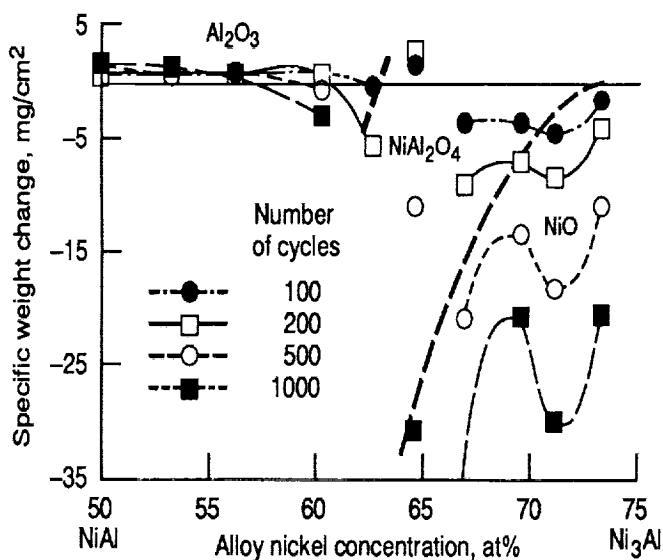


Figure 19. - Specific weight change versus intermetallic Ni content for the cyclic oxidation of Ni-Al-Zr alloys at 1473 K showing three different regions of behavior related to the primary oxide phase formed. (After Doychak et al. (ref. 182)).

While strides have been made in improving the room temperature ductility and toughness of NiAl-based materials, these advances have been at the expense of the original properties which have made NiAl a high temperature material candidate. Future efforts will have to concentrate not only on improving the low temperature properties of NiAl, which has now been demonstrated, but on developing a well rounded structural alloy. The latter goal seems to have been lost in present studies of macrostructurally toughened NiAl alloys. But as section 5 briefly demonstrated, there are a limitless number of alloying and structural modifications which can be made to NiAl. Therefore, the likelihood is great that eventually the room temperature behavior of NiAl will be improved without severely degrading the intermetallics other beneficial properties.

## 7. Conclusions

1. At low temperatures, NiAl suffers from poor fracture toughness and inherently low ductility due to an insufficient number of independent slip systems to accommodate grain boundary compatibility.

2. In two phase alloys a continuous ductile phase surrounding NiAl grains may act as a compliant layer and restore mechanical compatibility to the material. This mechanism has been successful in increasing the toughness of NiAl-based materials though increases in ductility seem to be dependent on the type of film present.

3. The biggest improvements in low temperature behavior result from the presence of a continuous ductile phase in either fiber or lamellar form, with toughening attributed to crack bridging with additional contributions by crack blunting and crack deflection mechanisms.

4. When special orientation relationships exist between the NiAl matrix phase and the ductile phase, toughening also appears to be the result of strain transfer into the NiAl due to plastic deformation of the ductile phase. The amount of toughening attributed to this mechanism has not determined and may be impossible to separate from other toughening mechanisms, yet it significantly contributes to the enhanced plasticity of the  $\beta$ -phase by inhibiting crack nucleation.

5. It has been demonstrated that the ductility and toughness of NiAl-based materials can be improved through the incorporation of a ductile second phase. Presently, this has been accomplished at the expense of other properties e.g., creep resistance, oxidation resistance and density.

6. With all the NiAl-based systems available for investigation it is still hopeful that a material will eventually be developed with an adequate balance of properties suitable for high temperature structural applications.

## Acknowledgments

The authors would like to acknowledge I.E. Locci, J.D. Cotton and J.D. Whittenberger for allowing us to use currently unpublished results in this paper and A.D. Tenteris-Noebe and M.V. Nathal for helpful comments concerning this manuscript. The portions of the research conducted at The University of Michigan were funded by the National Science Foundation, Grant No. DMR-8810058.

## References

1. Bremer, F.J., et al.: Experimental Analysis of the Ni-Al Phase Diagram. J. Crystal Growth, vol. 87, 1988, pp. 185-192.



2. Booker, J.; Paine, P.M.; and Stinehouse, A.J.: Investigation of Intermetallic Compounds for Very High Temperature Applications. WADD TR-60-889, 1961.
3. High Temperature Ordered Intermetallic Alloys, Vols. I-IV. MRS Symposium Proceedings, Pittsburgh, PA., Vol. I, 1985; Vol. II, 1987; Vol. III, 1988; Vol. IV, 1991.
4. Coons, L.: Advanced Materials for Future High Speed Civil Transport. HITEMP Review 1989, NASA CP-10039, 1989, pp. 5-1 to 5-12.
5. Darolia, R.; Field, R.D.; and Lahrman, D.F.: Alloy Modelling and Experimental Correlation for Ductility Enhancement in Near Stoichiometric Single Crystal Nickel Aluminide. AFOSR Contract F49620-88-C-0052, 1989.
6. Grala, E.M.: Investigation of the NiAl Phase of Nickel-Aluminum Alloys. NACA TN-3828, 1957.
7. Wood, D.L.; and Westbrook, J.H.: Effect of Basic Physical Parameters on Engineering Properties of Intermetallic Compounds. WADD TR-60-184, 1960. (Avail. NTIS, AD-246540).
8. Dobbs, J.; (General Electric Aircraft Engine Group) and Nathal, M.V.; and Noebe, R.D.: (NASA Lewis Research Center), Unpublished Research. 1990.
9. Taylor, R.E.; Groot, H.; and Larimore, J.: Thermophysical Properties of Aluminides. TPRL-506, Purdue University, West Lafayette, IN, 1986.
10. Harmouche, M.R.; and Wolfenden, A.: Modulus Measurements in Ordered Co-Al, Fe-Al, and Ni-Al Alloys. J. Test. Eval., vol. 13, 1985, pp. 424-428.
11. Hellmann, J.R., et al.: Interfacial Shear Studies in Sapphire-Fiber Reinforced Niobium and Nickel Aluminide Composites. HITEMP Review 1990, NASA CP-10051, 1990, pp. 41-1 to 41-11.
12. Singleton, R.H.; Wallace, A.V.; and Miller, D.G.: Nickel Aluminide Leading Edge for a Turbine Vane. Summary of the Eleventh Refractory Composites Working Group Meeting, E.H. Beardslee and D.R. James, eds., AFML-TR-66-179, 1966, pp. 717-739.
13. Rybicki, G.C.; and Smialek, J.L.: Effect of the Theta-Alpha-Al<sub>2</sub>O<sub>3</sub> Transformation on the Oxidation Behavior of Beta-NiAl+Zr. Oxid. Met., vol. 31, 1989, pp. 275-304.
14. Doychak, J.; Smialek, J.L.; and Barrett, C.A.: The Oxidation of Ni-Rich NiAl Intermetallics. Oxidation of High-Temperature Intermetallics, T. Grobstein and J. Doychak, eds., The Minerals, Metals & Materials Society, Warrendale, PA, 1989, pp. 41-55.
15. Barrett, C.A.: Effect of 0.1 At % Zirconium on the Cyclic Oxidation Resistance of Beta-NiAl. Oxid. Met., vol. 30, 1988, pp. 361-390.
16. Lowell, C.E.; Barrett, C.A. and Whittenberger, J.D.: Cyclic Oxidation Resistance of a Reaction Milled NiAl-AlN Composite. Intermetallic Matrix Composites, D.L. Anton, et al., eds., MRS Symposium Proceedings Vol. 194, Pittsburgh, PA, 1990, pp. 355-360.
17. Darolia, R.: NiAl Alloys for High-Temperature Structural Applications. J. of Metals, vol. 43, no. 3, 1991, pp. 44-49.
18. Whittenberger, J.D.; Arzt, E.; and Luton, M.J.: Preliminary Investigation of a NiAl Composite Prepared by Cryomilling. J. Mater. Res., vol. 5, 1990, pp. 271-277.
19. Whittenberger, J.D.; Arzt, E.; and Luton, M.J.: 1300 K Compressive Properties of a Reaction Milled NiAl-AlN Composite. J. Mater. Res., vol. 5, 1990, pp. 2819-2827.
20. Whittenberger, J.D.; and Noebe, R.D.: to be published (1991).
21. Wasilewski, R.J.; Butler, S.R.; and Hanlon, J.E.: Plastic Deformation of Single-Crystal NiAl. Trans. Metall. Soc. AIME, vol. 239, 1967, pp. 1357-1364.
22. Strutt, P.R.; Dodd, R.A.; and Rowe, G.M.: Creep in Stoichiometric Beta-NiAl. Strength of Metals and Alloys, Vol. III, ASM International, Metals Park, OH, 1970, pp. 1057-1061.
23. Pascoe, R.T.; and Newey, C.W.A.: Deformation Modes of Intermediate Phase NiAl. Phys. Stat. Sol., vol. 29, 1968, pp. 357-366.
24. Kanne, W.R.; Strutt, P.R.; and Dodd, R.A.: Nature of Slip Line and Substructure Formation During Creep in Stoichiometric NiAl at Temperatures Between 475° and 775 °C. Trans. Metall. Soc. AIME, vol. 245, 1969, pp. 1259-1267.
25. Loretto, M.H.; and Wasilewski, R.J.: Slip Systems in NiAl Single Crystals at 300 °K and 77 °K. Philos. Mag., vol. 23, 1971, pp. 1311-1328.
26. Bevk, J.; Dodd, R.A.; and Strutt, P.R.: The Orientation Dependence of Deformation Mode and Structure in Stoichiometric NiAl Single Crystals Deformed by High Temperature Steady State Creep. Metall. Trans., vol. 4, 1973, pp. 159-166.
27. Fraser, H.L.; Smallman, R.E.; and Loretto, M.H.: The Plastic Deformation of NiAl Single Crystals Between 300 K and 1050 K. I-Experimental Evidence on the Role of Kinking and Uniform Deformation in Crystals Compressed Along the 001 Direction. Philos. Mag., vol. 28, 1973, pp. 651-665.
28. Fraser, H.L.; Loretto, M.H.; and Smallman, R.E.: The Plastic Deformation of NiAl Single Crystals Between 300 K and 1050 K. II - The Mechanism of Kinking and Uniform Deformation. Philos. Mag., vol. 28, 1973, pp. 667-677.
29. Loretto, M.H.; and Wasilewski, R.J.: Strength of Metals and Alloys, Vol. I, ASM International, Metals Park, OH, 1970, pp. 113-117.
30. Field, R.D.; Lahrman, D.F.; and Darolia, R.: Room Temperature Deformation in "Soft" Orientation NiAl Single Crystals. High Temperature Ordered Intermetallic Alloys IV, L. Johnson, et al., eds., MRS Symp. Proc. Vol. 213, Pittsburgh, PA, 1991, pp. 225-260.

31. Ball, A.; and Smallman, R.E.: The Operative Slip System and Genral Plasticity of NiAl-II. *Acta Metall.*, vol. 14, 1966, pp. 1517-1526.
32. Kim, J.-T.: On the Slip Behavior and Surface Film Effects in B2 Ordered NiAl Single Crystals. Ph.D. Thesis, The University of Michigan, 1990.
33. Bowman, R.R.; Noebe, R.D.; and Darolia, R.: Mechanical Properties and Deformation Mechanisms of NiAl. HITEMP Review 1989, NASA CP-10039, 1989, pp. 47-1 to 47-15.
34. Zaluzec, N.J.; and Fraser, H.L.: The Origin of Dislocations With  $\mathbf{b} = \langle 110 \rangle$  in Single Crystals of  $\beta$ -NiAl Compressed Along  $\langle 001 \rangle$  at Elevated Temperatures. *Scr. Metall.*, vol. 8, 1974, pp. 1049-1053.
35. Kim, J.T.; and Gibala, R.: Slip Transition in  $[001]$  Oriented NiAl at High Temperatures. High Temperature Ordered Intermetallic Alloys IV, L. Johnson, et al., eds., MRS Symp. Proc. Vol. 213, Pittsburgh, PA, 1991, pp. 261-266.
36. Kim, J.T.; Noebe, R.D.; and Gibala, R.: Observation of Dislocation Substructures in Surface Oxide Softened Single Crystals of NiAl. Intermetallic Compounds-Structure and Mechanical Properties, Proc. 6th JIM Int. Symp., Japanese Institute of Metals, 1991, to be published.
37. Strutt, P.R., et al.: Creep in Ordered Binary and Ternary Ordered B.C.C. Alloys. Electron Microscopy and Structure of Materials, G. Thomas, ed., University of California Press, Berkeley, CA, 1972, pp. 722-731.
38. Lautenschlager, E.P.; Tisone, T.C.; and Brittain, J.O.: Electron Transmission Microscopy of NiAl. *Phys. Stat. Sol.*, vol. 20, 1967, pp. 443-450.
39. Vedula, K.; Hahn, K.H.; and Boulogne, B.: Room Temperature Tensile Ductility in Polycrystalline B2-NiAl. High Temperature Ordered Intermetallic Alloys III, C.T. Liu, et al., eds., MRS Symp. Proc. Vol. 133, Pittsburgh, PA, 1989, pp. 299-304.
40. Bowman, R.R., et al.: Correlation of Deformation Mechanisms With the Tensile and Compressive Behavior of NiAl and NiAl[Zr] Intermetallic Alloys. Submitted to *Metall. Trans.*, 1991.
41. Noebe, R.D., et al.: The Potential for Ductility Enhancement from Surface and Interface Dislocation Sources in NiAl. High Temperature Aluminides and Intermetallics, S.H. Whang, et al., eds., The Minerals, Metals & Materials Society, Warrendale, PA, 1990, pp. 271-300.
42. Potter, D.I.: Prediction of the Operative Slip System in CsCl Type Compounds Using Anisotropic Elasticity Theory. *Mater. Sci. Eng.*, vol. 5, 1969, pp. 201-209.
43. Mendiratta, M.G.; and Law, C.C.: Dislocation Energies and Mobilities in B2-Ordered Fe-Al Alloys. *J. Mater. Sci.*, vol. 22, 1987, pp. 607-611.
44. Fu, C.L.; and Yoo, M.H.: First-Principles Investigation of Mechanical Properties of Mechanically Alloyed NiAl. High Temperature Ordered Intermetallic Alloys IV, L. Johnson, et al., eds., MRS Symp. Proc. Vol. 213, Pittsburgh, PA, 1991, pp. 667-672.
45. Groves, G.W.; and Kelly, A.: Independent Slip Systems in Crystals. *Philos. Mag.*, vol. 8, 1963, pp. 877-887.
46. von R.V. Mises: Mechanik der Plastischen Formanderung von Kristallen. *Z. Angew. Math. Mech.*, vol. 8, 1928, pp. 161-185.
47. Noebe, R.D., et al.: Flow and Fracture Behavior of NiAl in Relation to the Brittle-to-Ductile Transition Temperature. High Temperature Ordered Intermetallic Alloys IV, L. Johnson, et al., eds., MRS Symp. Proc. Vol. 213, Pittsburgh, PA, 1991, pp. 589-596.
48. Rozner, A.G.; and Wasilewski, R.J.: Tensile Properties of NiAl and NiTi. *J. Inst. Met.*, vol. 94, 1966, pp. 169-175.
49. Hahn, K.H.; and Vedula, K.: Room Temperature Tensile Ductility in Polycrystalline B2 NiAl. *Scr. Metall.*, vol. 23, 1989, pp. 7-12.
50. George, E.P.; and Liu, C.T.: Brittle Fracture and Grain Boundary Chemistry of Microalloyed NiAl. *J. Mater. Res.*, vol. 5, 1990, pp. 754-762.
51. Noebe, R.D.; et al.: Flow and Fracture Behavior of Binary NiAl with Prospects for Future Alloy Development. HITEMP Review - 1990, NASA CP-10051, 1990, pp. 20-1 to 20-19.
52. Nagpal, P.; and Baker, I.: The Effect of Grain Size on the Room Temperature Ductility of NiAl. *Scr. Metall. Mater.*, vol. 24, 1990, pp. 2381-2384.
53. Ball, A.; and Smallman, R.E.: The Deformation Properties and Electron Microscopy Studies of the Intermetallic Compound NiAl. *Acta Metall.*, vol. 14, 1966, pp. 1349-1355.
54. Zeller, M.V.; Noebe, R.D.; and Locci, I.E.: Grain Boundary Segregation Studies of NiAl and NiAl(Zr) Using AES. HITEMP Review - 1990, NASA CP-10051, 1990, pp. 21-1 to 21-17.
55. Lahrman, D.F.; Field, R.D.; and Darolia, R.: The Effect of Strain Rate on the Mechanical Properties of Single Crystal NiAl. High Temperature Ordered Intermetallic Alloys IV, L. Johnson, et al., eds., MRS Symp. Proc. Vol. 213, Pittsburgh, PA, 1991, pp. 603-608.
56. Darolia, R., et al.: Alloy Modeling and Experimental Correlation for Ductility Enhancement in NiAl. High Temperature Ordered Intermetallic Alloys III, C.T. Liu, et al., eds., MRS Symp. Proc. Vol. 133, Pittsburgh, PA, 1989, pp. 113-118.
57. Lewandowski, J.J.; Michal, G.M.; Locci, I.E.; and Rigney, J.D.: Fracture Toughness and the Effects of Stress State on Fracture of Nickel Aluminides. Alloy Phase Stability and Design, G.M. Stocks, et al., eds., MRS Symp. Proc. Vol. 186, Pittsburgh, PA, 1990, to appear.
58. Kumar, K.S., et al.: Nickel Aluminide/Titanium Diboride Composites Via XD<sup>TM</sup> Synthesis. MML-TR-89-102(C), Martin Marietta Labs, 1989, p. 25.

59. Russell, S.M., et al.: Lightweight Disk Alloy Development, FR-19577-8, Pratt and Whitney, 1989, p. 30.
60. Reuss, S.; and Vehoff, H.: Temperature Dependence of the Fracture Toughness of Single Phase and Two Phase Intermetallics. *Scr. Metall. Mater.* vol. 24, 1990, pp. 1021-1026.
61. Sauthoff, G.: Mechanical Properties of Intermetallics at High Temperatures. High Temperature Aluminides and Intermetallics, S.H. Whang, et al., eds., The Minerals, Metals & Materials Society, Warrendale, PA, 1990, pp. 329-352.
62. Kazmin, V.I.; Mileiko, S.T.; and Tvardovsky, V.V.: Strength of Ceramic Matrix-Metal Fibre Composites *Compos. Sci. Technol.* vol. 38, 1990, pp. 69-84.
63. Chang, K.-M.; Darolia, R.; and Lipsitt, H.A.: Fracture of B2 Aluminide Single Crystals. High Temperature Ordered Intermetallic Alloys IV, L. Johnson, et al., eds., MRS Symp. Proc. Vol. 213, Pittsburgh, PA, 1991, pp. 597-602.
64. Raj, S.V.; Noebe, R.D.; and Bowman, R.: Observations on the Brittle to Ductile Transition Temperatures of B2 Nickel Aluminides With and Without Zirconium. *Scr. Metall.*, Vol. 23, 1989, pp. 2049-2054.
65. Mason, D.P., et al.: Microstructure and Mechanical Properties of Near Eutectic  $\beta$ -NiAl Plus  $\alpha$ -Re Alloys Produced by Rapid Solidification and Extrusion. High Temperature Ordered Intermetallic Alloys IV, L. Johnson, et al., eds., MRS Symp. Proc. Vol. 213, Pittsburgh, PA, 1991, pp. 1033-1038.
66. Groves, G.W.; and Kelly, A.: Change of Shape Due to Dislocation Climb. *Philos. Mag.*, vol. 19, 1969, pp. 977-986.
67. Law, C.C.; and Blackburn, M.J.: Rapidly Solidified Lightweight Durable Disk Material. AFWAL-TR-87-4102, 1987. (Avail. NTIS, AD-A191697).
68. Krstic, V.D.; Nicholson, P.S.; and Hoagland, R.G.: Toughening of Glasses by Metallic Particles. *J. Am. Ceram. Soc.*, vol. 64, 1981, pp. 499-504.
69. Sigl, L.S.; and Exner, H.E.: Experimental Study of the Mechanics of Fracture in WC-Co Alloys. *Metall. Trans. A*, vol. 18, 1987, pp. 1299-1308.
70. Sigl, L.S., et al.: On the Toughness of Brittle Materials Reinforced With a Ductile Phase. *Acta Metall.*, vol. 36, 1988, pp. 945-953.
71. Newkirk, M.S.; et al.: Formation of Lanthanide Ceramic Composite Materials. *J. Mater. Res.*, vol. 1, 1986, pp. 81-89.
72. Flinn, B.D.; Ruhle, M.; and Evans, A.G.: Toughening in Composites of  $Al_2O_3$  Reinforced With Al. *Acta Metall.*, vol. 37, 1989, pp. 3001-3006.
73. Hing, P.; and Groves, G.W.: The Strength and Fracture Toughness of Polycrystalline Magnesium Oxide Containing Metallic Particles and Fibres. *J. Mater. Sci.*, vol. 7, 1972, pp. 427-434.
74. Odette, G.R.; et al.: The Influence of the Reaction Layer Structure and Properties on Ductile Phase Toughening in Titanium Aluminide-Niobium Composites. *Interfaces in Metal-Ceramics Composites*, R.Y. Lin, et al., eds., The Minerals, Metals & Materials Society, Warrendale, PA, 1989, pp. 443-464.
75. Evans, A.G.: Perspective on the Development of High-Toughness Ceramics. *J. Am. Ceram. Soc.*, vol. 73, 1990, pp. 187-206.
76. Nardone, V.C.; and Strife, J.R.: NiAl-Based Microstructurally Toughened Composites. *Metall. Trans. A*, Vol. 22, 1991, pp. 183-189.
77. Evans, A.G.; He, M.Y.; and Hutchinson, J.W.: Interface Debonding and Fiber Cracking in Brittle Matrix Composites. *J. Am. Ceram. Soc.*, vol. 72, 1989, pp. 2300-2303 (also Evans, A.G.; and Marshall, D.B.: The Mechanical Behavior of Ceramic Matrix Composites. *Acta Metall.*, vol. 37, 1989, pp. 2567-2583).
78. Newkirk, J.W.; and Sago, J.A.: Ductile Phase Toughening of  $Cr_3Si$  with Chromium. *Intermetallic Matrix Composites*, D.L. Anton, et al., eds., MRS Symp. Proc. Vol. 194, Pittsburgh, PA, 1990, pp. 183-190.
79. Xiao, L.; Kim, Y.S.; and Abbaschian, R.: Ductile Phase Toughening of  $MoSi_2$  Chemical Compatibility and Fracture Toughness. *Intermetallic Matrix Composites*, D.L. Anton, et al., eds., MRS Symp. Proc. Vol. 194, Pittsburgh, PA, 1990, pp. 399-404.
80. Lu, L.; et al.: Reactive Synthesis of  $NbAl_3$  Matrix Composites. *Intermetallic Matrix Composites*, D.L. Anton, et al., eds., MRS Symp. Proc. Vol. 194, Pittsburgh, PA, 1990, pp. 79-88.
81. Lewandowski, J.J., et al.: Microstructural Effects on Ductile Phase Toughening of Nb-Nb Silicide Composites. High Temperature/High Performance Composites, F.D. Lemkey, et al., eds., MRS Symposium Proceedings Vol. 120, Pittsburgh, PA, 1988, pp. 103-109.
82. Nekkanti, R.M.; and Dimiduk, D.M.: Ductile Phase Toughening in Niobium-Niobium Silicide Powder Processed Composites. *Intermetallic Matrix Composites*, D.L. Anton, et al., eds., MRS Symp. Proc. Vol. 194, Pittsburgh, PA, 1990, pp. 175-182.
83. Subramanian, P.R., et al.: Microstructures and Mechanical Properties of NiAl+Mo In Situ Eutectic Composites. *Intermetallic Matrix Composites*, D.L. Anton, et al., eds., MRS Symp. Proc. vol. 194, Pittsburgh, PA, 1990, pp. 147-154.
84. Elliot, C.K. et al.: Toughening Mechanisms in Intermetallic Gamma-TiAl Alloys. High Temperature/High Performance Composites, F.D. Lemkey, et al., eds., MRS Symp. Proc. vol. 120, Pittsburgh, PA, 1988, pp. 95-101.
85. Rowe, R.G.: Recent Developments in Ti-Al-Nb Titanium Aluminide Alloys. High Temperature Aluminides and Intermetallics, S.H. Whang, et al., eds., The Minerals, Metals & Materials Society, Warrendale, PA, 1990, pp. 375-401.

86. Nishiyama, Y. et al.: Development of Titanium Aluminide Turbocharger Rotors. High Temperature Aluminides and Intermetallics, S.H. Whang, et al., eds., The Minerals, Metals & Materials Society, Warrendale, PA, 1990, pp. 557-584.
87. Lukasak, D.A.; and Koss, D.A.: The Flow and Fracture of  $Ti_3Al$ -Nb Alloy. Metall. Trans. A, vol. 21, 1990, pp. 135-143.
88. Chan, K.S.: Fracture and Toughening Mechanisms in an Alpha-2 Titanium Aluminide Alloy. Metall. Trans. A, vol. 21, 1990, pp. 2687-2699.
89. Aswath, P.B.; and Suresh, S.: Fatigue Crack Growth Behavior of a Titanium Aluminide Intermetallic. Mater. Sci. Eng. A, vol. 114, 1989, pp. L5-L10.
90. Blackburn, M.J.; and Smith, M.P.: Improved Toughness Alloys Based On Titanium Aluminides. WRDC-TR-89-4095, 1989. (Avail. NTIS, AD-A218149).
91. Sastry, S.M.L.; and Lipsitt, H.A.: Ordering Transformations and Mechanical Properties of  $Ti_3Al$  and  $Ti_3Al$ -Nb Alloys. Metall. Trans. A, vol. 8, 1977, pp. 1543-1552.
92. Lipsitt, H.A.; Shechtman, D.; and Schafrik, R.E.: The Deformation and Fracture of  $Ti_3Al$  at Elevated Temperatures. Metall. Trans. A, vol. 11, 1980, pp. 1364-1375.
93. Shen, Z.; Wagoner, R.H.; and Clark, W.A.T.: Dislocation and Grain Boundary Interactions in Metals. Acta Metall., vol. 36, 1988, pp. 3231-3242.
94. Lee, T.C.; Robertson, I.M.; and Birnbaum, H.K.: TEM Insitu Deformation Study of the Interaction of Lattice Dislocations With Grain Boundaries in Metals. Philos. Mag., vol. 62, 1990, pp. 131-153.
95. Lee, T.C.; Robertson, I.M.; and Birnbaum, H.K.: An Insitu Transmission Electron Microscope Deformation Study of the Slip Transfer Mechanisms in Metals. Metall. Trans. A, vol. 21, 1990, pp. 2437-2447.
96. Lee, T.C.; Robertson, I.M.; and Birnbaum, H.K.: Prediction of Slip Transfer Mechanisms Across Grain Boundaries. Scr. Metall., vol. 23, 1989, pp. 799-803. (Correction; p. 1467.)
97. Carrington, W.E.; and McLean, D.: Slip Nuclei in Silicon-Iron. Acta Metall., vol. 13, 1965, pp. 493-499.
98. Bond, G.M.; Robertson, I.M.; and Birnbaum, H.K.: Effect of Boron on the Mechanism of Strain Transfer Across Grain Boundaries in  $Ni_3Al$ . J. Mater. Res., vol. 2, 1987, pp. 436-440.
99. Singleton, M.F.; Murray, J.L.; and Nash, P.: Al-Ni (Aluminum-Nickel). Binary Alloy Phase Diagrams, T.B. Massalski, ed., American Society for Metals, Metals Park, OH, 1986, pp. 140, 142-143.
100. Dulmaine, B.: Stability and Kinetics of Formation of  $Ni_3Al$  in a Nickel Aluminide Alloy. Fall TMS meeting, Indianapolis, IN, Oct. 1989.
101. Khadkikar, P.S.; Locci, I.E.; Vedula, K.; and Michal, G.M.: Transformation to  $Ni_3Al$  in a 63.0 at % Ni-Al Alloy. submitted to Metall. Trans., 1991.
102. Schramm, J.: The Binary System Ni-NiAl. Z. Metallk., vol. 33, 1941, pp. 347-355.
103. Ritzert, F.J.; Noebe, R.D.; and Nathal, M.V.: The Effect of Processing and Discontinuous Reinforcement on the Properties of a Powder Metallurgy Extruded Two Phase  $\beta+\gamma$  Nickel Aluminide. to be published
104. Noebe, R.D.: NASA Lewis Research Center, unpublished data.
105. Nourbakhsh, S.; and Chen, P.: Microstructure and Mechanical Properties of Rapidly Solidified and Annealed NiAl Intermetallic Alloys. Acta Metall., vol. 37, 1989, pp. 1573-1583.
106. Tewari, S.N.: Directionally Solidified Eutectic Alloy Gamma-Beta. NASA TN D-8355, 1977.
107. Ishida, K., et al.: Ductility Enhancement in NiAl(B2)-Base Alloys by Microstructural Control. Metall. Trans. A, vol. 22, 1991, pp. 441-446.
108. Pank, D.R.; Nathal, M.W.; and Koss, D.A.: Microstructure and Mechanical Properties of Multiphase NiAl-Based Alloys. J. Mater. Res., vol. 5, 1990, pp. 942-949.
109. Pank, D.R.: The Effect of Alloying on the Microstructure and Mechanical Properties of Rapidly Solidified Ni-Al Alloys. M.S. Thesis, Pennsylvania State University, 1988.
110. Inoue, A.; Masumoto, T.; and Tomioka, H.: Microstructure and Mechanical Properties of Rapidly Quenched  $L2_0$  and  $L2_0+L1_2$  Alloys in Ni-Al-Fe and Ni-Al-Co Systems. J. Mater. Sci., vol. 19, 1984, pp. 3097-3106.
111. Inoue, A., et al.: Microstructure and Mechanical Properties of Ductile Intermetallic Compounds Produced by Melt Quenching. Int. J. Rapid Solid., vol. 1, 1985, pp. 115-142.
112. Moskovic, R.: Mechanical Properties of Precipitation-Strengthened Ni-Al-Cr Alloy Based on an NiAl Intermetallic Compound. J. Mater. Sci., vol. 13, 1978, pp. 1901-1906.
113. Baldan, A.; and West, D.R.F.: Structural Features of Certain Ni-Al-Ta and Ni-Al-Hf Alloys Containing the Gamma Prime and Beta Phases. J. Mater. Sci., vol. 16, 1981, pp. 24-34.
114. Huang, S.C.; Field, R.D.; and Krueger, D.D.: Microscopy and Tensile Behavior of Melt-Spun Ni-Al-Fe Alloys. Metall. Trans. A, vol. 21, 1990, pp. 959-970.
115. Larsen, M., et al.: Ductility Enhancement from Interface Dislocation Sources in a Directionally Solidified Beta ((Gamma + Gamma') Ni-Fe-Al Composite Alloy). Intermetallic Matrix Composites, D.L. Anton, et al., eds., MRS Symp. Proc. vol. 194, Pittsburgh, PA, 1990, pp. 191-198.
116. Guha, S.; Munroe, P.R.; and Baker, I.: Room Temperature Deformation Behavior of Multiphase Ni-20 at % Al-30 at % Fe and its Constituent Phases. Mater. Sci. Eng. A, vol. 131, 1991, pp. 27-38.

117. Copley, S.M.; and Kear, B.H.: A Dynamic Theory of Coherent Precipitation Hardening with Application to Nickel-Base Superalloys. *Metall. Soc. AIME Trans.*, vol. 239, 1967, pp. 984-992.
118. Izumi, O.; and Takasugi, T.: Deformability Improvements of L1(2)-Type Intermetallic Compounds. High Temperature Ordered Intermetallic Alloys II, N.S. Stoloff, et al., eds., MRS Symp. Proc. Vol. 81, Pittsburgh, PA, 1987, pp. 173-182.
119. Aoki, K.; and Izumi, O.: Improvement in Room Temperature Ductility of the L12 Type Intermetallic Compound Ni<sub>3</sub>Al by Boron Addition. *J. Jpn. Inst. Met.*, vol. 43, 1979, pp. 1190-1196.
120. Pope, D.P.: Dislocation Mechanisms and Anomalous Flow in L1<sub>2</sub> Alloys. High Temperature Aluminides and Intermetallics, S.H. Whang, et al., eds., The Minerals, Metals & Materials Society, Warrendale, PA, 1990, pp. 51-61.
121. Reynaud, F.: Mise en Evidence Par Diffraction Electronique de la Mise en Ordre des Atomes de Nickel en Exces par Rapport a la Stoechiometrie dans les Alliages  $\beta'$ -NiAl Riches en Nickel: Formation d'une Surstructure Ni<sub>2</sub>Al. *J. Appl. Cryst.*, vol. 9, 1976, pp. 263-268.
122. Locci, I.E., et al.: Compendium of Alloy Phases Observed After Low Temperature Aging of Ni-Rich NiAl. *Proc. XII Int. Cong. for Electron Microscopy*, San Francisco Press, Inc., San Francisco, CA, 1990, pp. 944-945.
123. Robertson, I.M.; and Wayman, C.M.: Ni<sub>3</sub>Al<sub>3</sub> and the Nickel-Aluminum Binary Phase Diagram. *Metallography*, vol. 17, 1984, pp. 43-55.
124. Smialek, J.L.; and Hehemann, R.F.: Transformation Temperatures of Martensite in Beta-Phase Nickel Aluminide. *Metall. Trans.*, vol. 4, 1973, pp. 1571-1575.
125. Litvinov, V.S.; Zelenin, L.P.; and Shklyar, R.S.: Diffusionless Transformation in Ni-Al Alloys With a Caesium Chloride Lattice. *Fiz. Metal. Metalloved.*, vol. 31, 1971, pp. 138-142.
126. Au, Y.K.; and Wayman, C.M.: Thermoelastic Behavior of the Martensitic Transformation in  $\beta'$  NiAl Alloys. *Scripta Metall.*, vol. 6, 1972, pp. 1209-1214.
127. Ochiai, S.; and Ueno, M.: Composition Dependence of the M<sub>s</sub> Temperature in the Beta' NiAl Compound. *J. Inst. Met.*, vol. 52, 1988, pp. 157-162 (NASA TT-20336).
128. Chakravorty, S.; and Wayman, C.M.: The Thermoelastic Martensitic Transformation in Beta-Prime Ni-Al Alloys. *Metall. Trans. A*, vol. 7, 1976, pp. 555-582.
129. Kim, Y.D.; and Wayman, C.M.: Shape Memory Effect in Powder Metallurgy NiAl Alloys. *Scr. Metall. Mater.*, vol. 24, 1990, pp. 245-250.
130. Khadkikar, P.S.; Vedula, K.; and Shabel, B.S.: Two-Phase Nickel Aluminides. High Temperature Ordered Intermetallic Alloys II, N.S. Stoloff, et al., eds., MRS Symp. Proc. Vol. 81, Pittsburgh, PA, 1987, pp. 157-164.
131. Russell, S.M.; Law, C.C.; and Blackburn, M.J.: The Effect of Cobalt on Martensitic Toughening Parameters in NiAl. High Temperature Ordered Intermetallic Alloys III, C.T. Liu, et al., eds., MRS Symp. Proc. Vol. 133, Pittsburgh, PA, 1989, pp. 627-632.
132. Antolovich, S.D.; and Fahr, D.: An Experimental Investigation of the Fracture Characteristics of Trip Alloys. *Eng. Fract. Mech.*, vol. 4, 1972, pp. 133-144.
133. Evans, A. G.; and Heuer, A.H.: Transformation Toughening in Ceramics - Martensitic Transformations in Crack-Tip Stress Fields. *J. Am. Ceram. Soc.*, vol. 63, 1980, pp. 241-248.
134. McMeeking, R.; and Evans, A.G.: Mechanics of Transformation-Toughening in Brittle Materials. *J. Am. Ceram. Soc.*, vol. 65, 1982, pp. 242-246.
135. Swain, M.W.: Inelastic Deformation of Mg-PSZ and its Significance for Strength-Toughness Relationship of Zirconia Toughened Ceramics. *Acta Metall.*, vol. 33, 1985, pp. 2083-2091.
136. Lange, F.F.: Transformation Toughening. Part 1 - Size Effects Associated with the Thermodynamics in Constrained Transformations. *J. Mater. Sci.*, vol. 17, 1982, pp. 225-234.
137. Kelly, P.M.; and Ball, C.J.: Crystallography of Stress-Induced Martensitic Transformations in Partially Stabilized Zirconia. *J. Am. Ceram. Soc.*, vol. 69, 1986, pp. 259-264.
138. Lange, F.F.: Transformation Toughening. Part 4 - Fabrication, Fracture Toughness and Strength of Al<sub>2</sub>O<sub>3</sub>-ZrO<sub>2</sub> Composites. *J. Mater. Sci.*, vol. 17, 1982, pp. 247-254.
139. Russell, S.M.; and Law, C.C.: Nickel Aluminide Materials Having Toughness and Ductility at Low Temperatures, US Patent 4,961,905, 1990.
140. Russell, K.C.; and Edington, J.W.: Precipitation Behaviour and Mechanical Properties of a Nickel-36 at. % Aluminum Alloy. *Met. Sci. J.*, vol. 6, 1972, pp. 20-24.
141. Moskovic, R.: Precipitation of Ni<sub>3</sub>Al in a Nickel Rich NiAl. *J. Mater. Sci.*, vol. 12, 1977, pp. 1895-1902.
142. Westbrook, J.H.: Temperature Dependence of Hardness of the Equi-Atomic Iron Group Aluminides. *J. Electrochem. Soc.*, vol. 103, 1956, pp. 54-63.
143. Vedula, K.; and Khadkikar, P.S.: Effect of Stoichiometry on Low Temperature Mechanical Properties of B2 NiAl Alloys. High Temperature Aluminides and Intermetallics, S.H. Whang, et al., eds., The Minerals, Metals & Materials Society, Warrendale, PA, 1990, pp. 197-217.
144. Heredia, F.E.; and Pope, D.P.: Solid Solution Strengthening of Ni<sub>3</sub>Al Single Crystals. Superalloys 1988, D.N. Duhal, et al., eds., The Metallurgical Society, Warrendale, PA, 1988, pp. 315-324.

145. Hartfield-Wunsch, S.: Monotonic and Cyclic Deformation of B2 Aluminides. Ph.D. Thesis, University of Michigan, 1991.
146. Hartfield-Wunsch, S.; and Gibala, R.: Cyclic Deformation of B2 Aluminides. High Temperature Ordered Intermetallic Alloys IV, L. Johnson, et al., eds., MRS Symp. Proc. vol. 213, Pittsburgh, PA, 1991, pp. 575-580.
147. Raj, S.V.; Noebe, R.D.; and Locci, I.E.: The Mechanical Properties of a Ni-30Al-20Fe-0.5Zr Intermetallic Alloy in the Temperature Range 300-1200 K. High Temperature Ordered Intermetallic Alloys IV, L. Johnson, et al., eds., MRS Symp. Proc. vol. 213, Pittsburgh, PA, 1991, pp. 673-678.
148. Cotton, J.D.: The Effect of Chromium Additions on the Room Temperature Plastic Deformation of  $\beta$ -NiAl. Ph.D. Thesis, University of Florida, in progress.
149. Raman, A.; and Schubert, K.: The Constitution of Some Alloy Series Related to TiAl<sub>3</sub>. III-Investigation on Some Ti-Ni-Al and Ti-Cu-Al Systems. Z. Metallkde., vol. 56, 1965, pp. 99-104.
150. Vedula, K., et al.: Alloys Based on NiAl for High Temperature Applications. High Temperature Ordered Intermetallic Alloys, C.C. Koch, et al., eds., MRS Symp. Proc. vol. 39, Pittsburgh, PA, 1985, pp. 411-421.
151. Field, R.D.; Darolia, R.; and Lahrman, D.F.: Precipitation in NiAl/Ni<sub>2</sub>AlTi Alloys. Scr. Metall., vol. 23, 1989, pp. 1469-1474.
152. Takeyama, M.; and Liu, C.T.: Microstructures and Mechanical Properties of NiAl-Ni<sub>2</sub>AlHf Alloys. J. Mater. Res., vol. 5, 1990, pp. 1189-1196.
153. Pellegrini, P.W.; and Hutta, J.J.: Investigations of Phase Relations and Eutectic Directional Solidification on the NiAl-V Join. J. Cryst. Growth, vol. 42, 1977, pp. 536-539.
154. Nash, P.; and Liang, W.W.: Phase Equilibria in the Ni-Al-Ti System at 1173 K. Metall. Trans. A., vol. 16, 1985, pp. 319-322.
155. Nash, P.G.; and Vejins, V.; and Liang, W.W.: Al-Ni-Ti. Bull. Alloy Phase Diagrams, vol. 3, 1982, pp. 374.
156. Polvani, R.S.; Tzeng, W.-S.; and Strutt, P.R.: High Temperature Creep in a Semi-Coherent NiAl-Ni<sub>2</sub>AlTi Alloy. Metall. Trans. A., vol. 7, 1976, pp. 33-40.
157. Pathare, V.M.: Processing, Physical Metallurgy and Creep of NiAl + Ta and NiAl + Nb Alloys. Ph.D. Thesis, Case Western Reserve University, 1988. (NASA CR-182113).
158. Oliver, B.: Containerless Processing of High Temperature Reactive Liquids. HITEMP Review-1989, NASA CP-10039, 1989, pp. 25-1 to 25-9.
159. Whittenberger, J.D.; Westfall, L.J.; and Nathal, M.V.: Compressive Strength of a B2 Matrix NiAl-Nb Intermetallic at 1200 and 1300 K. Scr. Metall., vol. 23, 1989, pp. 2127-2130.
160. Sherman, M.; and Vedula, K.: High Temperature Dispersion Strengthening of NiAl. J. Mater. Sci., vol. 21, 1986, pp. 1974-1980.
161. Walter, J.L.; and Cline, H.E.: The Effect of Solidification Rate on Structure and High Temperature Strength of the Eutectic NiAl-Cr. Metall. Trans., vol. 1, 1970, pp. 1221-1229.
162. Cline, H.E.; and Walter, J.L.: The Effect of Alloy Additions on the Rod-Plate Transition in the Eutectic NiAl-Cr. Metall. Trans., vol. 1, 1970, pp. 2907-2917.
163. Cline, H.E., et al.: Structures, Faults, and the Rod-Plate Transition in Eutectics. Metall. Trans., vol. 2, 1971, pp. 189-194.
164. Walter, J.L.; and Cline, H.E.: Stability of the Directionally Solidified Eutectics NiAl-Cr and NiAl-Mo. Metall. Trans., vol. 4, 1973, pp. 33-38.
165. Merchant, S.M.; and Notis, M.R.: A Review - Constitution of the Al-Cr-Ni System. Mater. Sci. Eng., vol. 66, 1984, pp. 47-60.
166. Stover, E.R.: Effects of Alloying and Deformation Processing on the Mechanical Behavior of NiAl. WADC-TDR-60-184, Part VII, Vol. II, 1966. (Avail. NTIS, AD-810645).
167. Webber, J.G.; and Van Aken, D.C.: Studies of a Quasi-Binary Beta-NiAl and Alpha-Re Eutectic. Scr. Metall., vol. 23, 1989, pp. 193-196.
168. Mason, D.P.; Van Aken, D.C.; and Webber, J.G.: Microstructural Studies of Beta-NiAl and Alpha-Re Composites Produced by Eutectic Solidification. Intermetallic Matrix Composites, D.L. Anton, et al., eds., MRS Symp. Proc. vol. 194, Pittsburgh, PA, 1990, pp. 341-348.
169. Budberg, P.B.: The Alloys of the Ternary System Nickel-Aluminum-Tungsten. J. Inorg. Chem. USSR, vol. 3, 1958, pp. 694-698.
170. Tietz, T.E.; and Wilson, J.W.: Behavior and Properties of Refractory Metals. Stanford University Press, 1965, pp. 352.
171. Bradley, A.J.; and Taylor, A.: An X-Ray Study of the Iron-Nickel-Aluminum Ternary Equilibrium Diagram. Proc. Roy. Soc. London Ser. A, vol. 166, 1938, pp. 353-375.
172. Rivlin, V.G.; and Raynor, G.V.: Phase Equilibria in Iron Ternary Alloys-2. Critical Evaluation of Constitution of Aluminum-Iron-Nickel System. Int. Met. Rev., vol. 25, 1980, pp. 79-93.
173. Alexander, W.O.: Copper-Rich Nickel-Aluminum-Copper Alloys. Pt. II - Constitution of Copper Nickel-Rich Alloys. J. Inst. Met., vol. 63, 1938, pp. 163-183.
174. Austin, C.R.; and Murphy, A.J.: The Ternary System Copper-Aluminum-Nickel. J. Inst. Met., vol. 29, 1923, pp. 327-378.

175. Chakravorty, S.; and West, D.R.F.: Phase Equilibria Between NiAl and RuAl in the Ni-Al-Ru System. *Scr. Metall.*, vol. 19, 1985, pp. 1355-1360.
176. Bradley, A.J.: Microscopical Studies on Iron-Nickel-Aluminum System. *J. Iron Steel Inst.*, vol. 163, 1949, pp. 19-30.
177. Koster, W.; Zwicker, U.; and Moeller, K.: Microscopic and X-Ray Investigations in the System Cu-Ni-Al. *Z. Metallkd.*, vol. 39, 1948, pp. 225-231.
178. Nardone, V.C.; Strife, J.R.; and Prewo, K.M.: Development of Highly Impact Resistant NiAl Matrix Composites. *Intermetallic Matrix Composites*, D.L. Anton, et al., eds., MRS Symp. Proc. Vol. 194, Pittsburgh, PA, 1990, pp. 205-210.
179. Bowman, R.R.; and Noebe, R.D.: Processing and Mechanical Evaluation of Continuous Fiber Reinforced NiAl Composites. *HITEMP Review - 1990*, NASA CP-10051, 1990, pp. 40-1 to 40-14.
180. Noebe, R.D.; Bowman, R.R.; and Eldridge, J.: Initial Evaluation of Continuous Fiber Reinforced NiAl Composites. *Intermetallic Matrix Composites*, D.L. Anton, et al., eds., MRS Symp. Proc. vol. 194, Pittsburgh, PA, 1990, pp. 323-332.
181. Patrician, T.J.; Sylvester, V.P.; and Daga, R.L.: High-Temperature P/M-Molybdenum Alloys. *Physical Metallurgy and Technology of Molybdenum and its Alloys*, K.H. Miska, et al., eds., AMAX Specialty Metals Corp., Greenwich CT, 1985, pp.1-11.
182. Doychak, J.; Barrett, C.A.; and Smialek, J.L.: Oxidation Between 100 °C and 1600 °C and Limiting Criteria for the Use of Zr-Doped Beta-NiAl and Gamma Prime Alloys. *Corrosion & Particle Erosion at High Temperatures*, V. Srinivasa and K. Vedula, eds., The Minerals, Metals & Materials Society, Warrendale, PA, 1989, pp. 487-514.
183. Shah, D.M.: Orientation Dependence of Creep Behavior of Single Crystal Gamma-Prime (Ni<sub>3</sub>Al). *Scr. Metall.*, vol. 17, 1983, pp. 997-1002.



National Aeronautics and  
Space Administration

## Report Documentation Page

1. Report No. NASA TM - 103796		2. Government Accession No.		3. Recipient's Catalog No.	
4. Title and Subtitle Prospects for Ductility and Toughness Enhancement of NiAl By Ductile Phase Reinforcement				5. Report Date July 1991	
				6. Performing Organization Code	
7. Author(s) R.D. Noebe, F.J. Ritzert, A. Misra, and R. Gibala				8. Performing Organization Report No. E - 6022	
				10. Work Unit No. 510 - 01 - 50	
9. Performing Organization Name and Address National Aeronautics and Space Administration Lewis Research Center Cleveland, Ohio 44135 - 3191				11. Contract or Grant No.	
				13. Type of Report and Period Covered Technical Memorandum	
12. Sponsoring Agency Name and Address National Aeronautics and Space Administration Washington, D.C. 20546 - 0001				14. Sponsoring Agency Code	
15. Supplementary Notes R.D. Noebe and F.J. Ritzert, NASA Lewis Research Center. A. Misra and R. Gibala, Department of Materials Science and Engineering, The University of Michigan, Ann Arbor, Michigan 41809 (work funded by the National Science Foundation Grant DMR - 8810058). Responsible person, R.D. Noebe, (216) 433 - 2093.					
16. Abstract <p>The use of NiAl as a structural material has been hindered by the fact that this ordered intermetallic does not exhibit significant tensile ductility or toughness at room temperature. A critical review of the operative flow and fracture mechanisms in monolithic NiAl has thus established the need for ductile phase toughening in this ordered system. Progress in ductile phase reinforced intermetallic systems in general and specifically NiAl-based materials has been reviewed. In addition, further clarification of the primary mechanisms involved in the flow and fracture of ductile phase reinforced alloys has evolved from ongoing investigations of several model NiAl-based materials. The mechanical behavior of these model directionally-solidified alloys (Ni-30Al and Ni-30Fe-20Al (at.%)) are discussed. Finally, the prospects for developing a ductile phase toughened NiAl-based alloy and the shortcomings presently inherent in these systems are analyzed.</p>					
17. Key Words (Suggested by Author(s)) Eutectic composites; Metal matrix composites; Intermetallics; Fracture strength; Ductility				18. Distribution Statement Unclassified - Unlimited Subject Category 26	
19. Security Classif. (of the report) Unclassified		20. Security Classif. (of this page) Unclassified		21. No. of pages 30	
				22. Price* A03	